March 1960

Technical Report 68

AERODYNAMIC CHARACTERISTICS OF TRAILING-WIRE ANTENNAS AT SUPERSONIC SPEEDS

By: F. B. Harris, Jr.

SRI Project 2494

Prepared for:

AIR FORCE CAMBRIDGE RESEARCH CENTER AIR RESEARCH AND DEVELOPMENT COMMAND
LAURENCE G. HANSCOM FIELD BEDFORD, MASSACHUSETTS

Contract AF 19(604)-3458

Approved:

S. B. COHN, MANAGER ELECTROMAGNETICS LABORATORY

D. R. SCHEUCH, ASSISTANT DIRECTOR OF ENGINEERING RESEARCH

Copy No.....35

ABSTRACT

Severe difficulties associated with the design of satisfactory flush-type HF transmitting antennas for supersonic aircraft have prompted a reconsideration of trailing-wire antennas for such vehicles. The aerodynamic instabilities which caused mechanical failure of the trailing-wire type of antenna and led to its abandonment except in low-speed applications are carefully examined in this report.

The shedding of a spiral vortex by the pear-shaped and spherical end-weights customarily used was primarily responsible for rotary motions which occurred at short cable lengths. This behavior can be eliminated through the use of a streamlined, , aerodynamically stable end-weight. To ensure that the antenna hangs down out of the turbulent boundary layer and wake of the aircraft, as well as to take the fullest possible advantage of the favorable electrical properties of the trailing wire, the end-weight should be relatively heavy and have as little aerodynamic drag as possible.

The phenomenon of aerodynamic wave amplification, which leads to violent mechanical cable oscillations in the vertical plane, is subjected to a comprehensive theoretical analysis. The partial differential equations of motion of the curved wire are shown to lead, in the case of harmonic time-dependence, to an approximate representation in terms of three waves. A general method is given for solving the boundary value problem in a given case. Simple analytic expressions are obtained for the total aerodynamic amplification of a traveling wave on the curved wire. The investigation shows that, although the amplification factor cannot be reduced to unity at supersonic speeds with wires of known materials and weights of practical sizes, it can nevertheless be held below dangerous levels.

The theory is applied to the computation of certain properties of an actual experimental trailing wire system which has been successfully flown at speeds up to Mach 1.24. An amplification factor of about 8 is indicated for the worst flight condition.

CONTENTS

CONTENTS

ILLUSTRATIONS

SYMBOLS

SYMBOL	DEFINITION
$A(\sigma_1, \sigma_2)$ $A_1(\sigma_1, \sigma_2)$	Total amplification of downstream wave from σ_2 to σ_1
$A_2(\sigma_1, \sigma_2)$	Total attenuation of upstream wave from σ_1 to σ_2
a	Amplitude of wave
a_1	Amplitude of downstream wave at origin
a_2	Amplitude of upstream wave at origin
a_0	Value of a at particular point
a_k	Coefficient of kth harmonic in Fourier expansion
B_n	Abbreviation for cofactor in determinant
b_1	Coefficient of u_1
b_2	Coefficient of u_2
b_k	Coefficient of kth harmonic in standing wave
C	Characteristic length of trailing cable
C_D	Drag coefficient of a cylinder
D	(1) Cable diameter (2) Abbreviation for determinant
F	Aerodynamic force
$f(s, t)$	Function defined by Eq. (B-7)
$f(\sigma)$	Abbreviation for $1 - 2i(\gamma/\nu)(1 + \sigma^2)^{-1/2}$
G	Dimensionless gravitational acceleration
g	(1) Gravitational acceleration (2) Amplitude deviation of u
h	Phase deviation of u
K	Non-aerodynamic damping constant

SYMBOL	DEFINITION
k	Aerodynamic growth or damping constant
m	Mass of end-weight
N	Dimensionless transverse displacement
N_1	Dimensionless transverse displacement (downstream wave)
N_2	Dimensionless transverse displacement (upstream wave)
N_0	Dimensionless transverse displacement at particular point
n	Transverse displacement
n_1	Transverse displacement (downstream wave)
n_2	Transverse displacement (upstream wave)
n_0	Transverse displacement at particular point
n_m	Maximum transverse displacement in standing wave
n_Σ	Transverse input amplitude applied at point Σ
P	Dimensionless longitudinal displacement
p	(1) Longitudinal displacement (2) Number of half-wave loops in standing wave
$q(\gamma)$	Function defined by Eq. (B-41)
r	Time-free fractional cable tension variation
S	Total cable length
S_0	Total undistorted cable length
s	Arc length along cable
s_0	Arc length along undistorted cable
T	Cable tension
T_0	Equilibrium value of T
t	Time
U	Wave propagation velocity
U_0	Wave propagation velocity in vacuo
u	$(1 + \sigma^2)^{1/2} w$
u_1	Homogenous solution for u (downstream wave)

SYMBOL	DEFINITION
u_2	Homogenous solution for u (upstream wave)
u_3	Particular integral for u
u_k	kth function in expansion of nonlinear solution
V_0	Free-stream air velocity
V_n	Component of air velocity normal to cable
γ	Time-free dimensionless longitudinal displacement
v_1, v_2, v_3	Functions defined by Eq. (46)
v_k	Function defined by Eq. (B-35)
v_{ki}	Imaginary part of v_k
v_{kr}	Real part of v_k
w	Time-free dimensionless transverse displacement
x	(1) Horizontal coordinate of point on cable (2) Real part of u_3 (3) Arbitrary independent variable
x_0	Equilibrium value of x
y	(1) Vertical coordinate of point on cable (2) Imaginary part of u_3, divided by $2\gamma\nu$
$y(x)$	$\lvert\sin x\rvert\sin x$
y_0	Equilibrium value of y
α	Angular deviation of cable at point
α_N	Dimensionless coefficient of viscous friction in N-direction
α_P	Dimensionless coefficient of viscous friction in P-direction
β	Fractional tension variation
γ	U/V_0
γ_0	U_0/V_0

SYMBOL	DEFINITION
ζ_N	Coupling constant in N-direction
ζ_P	Coupling constant in P-direction
η	Dimensionless vertical coordinate of point on cable
θ	Variable of integration
λ	Mechanical wavelength
μ	Mass of cable per unit length
μ_N	Coefficient of viscous friction in N-direction
μ_P	Coefficient of viscous friction in P-direction
ν	Dimensionless frequency
ν_N	Dimensionless natural frequency of end-weight and suspension in N-direction
ν_P	Dimensionless natural frequency of end-weight and suspension in P-direction
ξ	Dimensionless horizontal coordinate of point on cable
ρ	Air density
Σ	Total dimensionless cable length
Σ_0	Total dimensionless undistorted cable length
Σ'	Dimensionless amplitude of second-order length variation
σ	Dimensionless arc length along cable
σ_1	Dimensionless arc-length coordinate of lower end of cable
σ_2	Dimensionless arc-length coordinate of upper end of cable
σ_0	Dimensionless arc length along undistorted cable
τ	Dimensionless time
ϕ	Slope angle of cable
ϕ_0	Equilibrium value of ϕ
Φ	Slope angle of cable at lower end
ψ	Phase angle
ω	Angular frequency

AERODYNAMIC CHARACTERISTICS OF TRAILING-WIRE ANTENNAS AT SUPERSONIC SPEEDS

I INTRODUCTION

Most aircraft antennas for HF transmission act merely as coupling devices to excite currents on the airframe; the actual source of radiation is the airframe currents. This is true of tail and wing cap antennas, and such variants of these as wing, tail, and nose probe antennas.[1] It is also true of notch and shunt antennas, and even of fixed wires.[2,3]

With the evolution of the airplane through ever more sophisticated shapes to the delta-wing configuration, however, it has become increasingly difficult to design HF antenna systems capable of achieving adequate coupling. While on the one hand the new shapes have eliminated many of the natural charge and current concentrations necessary to obtain effective coupling, on the other hand the weight and structural penalties which can be tolerated have become ever smaller. Moreover, the drag associated with any external structure has risen greatly. The problem has been further complicated by the fact that, in the few remaining possible antenna locations, high ambient temperatures and limited space make extremely difficult, if not impossible, the design, housing, and maintenance of the often quite elaborate antenna couplers which are required.

These difficulties have prompted a reexamination of one of the older, more primitive types of antennas—the trailing wire. This antenna is different from the other antennas mentioned in that the wire itself is the principal radiating element.

Electrically, the trailing wire has many advantages over other types of HF antennas. One of the most important of these is that it can be tuned by simply varying the length. The magnitudes and degree of variation of the antenna impedances which are then seen at the feed point are such that very simple coupling arrangements will suffice. The radiation patterns

obtained are, in general, superior to those of the other antennas. In particular, if the end of the wire is properly weighted, the antenna can be made to hang down enough to give considerable vertical-dipole radiation, thus providing more nearly omni-azimuthal coverage. In addition, because the wire itself is the radiator, both patterns and impedance tend to be independent of the airframe on which it is installed. Although the antenna, when extended, contributes appreciable drag to the airplane, it can be retracted when not in use.

In spite of their electrical advantages, trailing wires, except for special low speed applications, were abandoned some years ago; at increased speeds aerodynamic instabilities set in, resulting in mechanical failure of the wires or, in some cases, damage to the aircraft. Since these instabilities were responsible for the abandonment of trailing wires, it is appropriate to examine possible causes for them to see whether they might not be eliminated. Investigation reveals two sources of instability which appear capable of accounting for the observed behavior.

In virtually all trailing-wire antenna installations until now, spherical or pear-shaped end-weights have been used. It is known from aerodynamic investigations that a sphere in a high-speed air stream sheds a spiral vortex.[4] The shedding of such a vortex by the spherical end-weight on a trailing wire tends to induce a rotary motion of the sphere. Depending on the length and tension of the wire a standing wave can be established on it, resulting in large amplitude rotary motions of the weight. Such motions have been observed in actual trailing wires. They occur as the wire is reeled in, sometimes causing the weight to pound against the bottom of the aircraft when the wire becomes short.

Equally serious as that just described is another form of instability which occurs when the speed of the aircraft exceeds the speed of propagation of mechanical waves on the wire. When this condition exists a wave traveling downstream on the wire will be amplified by aerodynamic action. This phenomenon was investigated by W. H. Phillips and others.[5,6] Phillips showed that the downstream wave will increase exponentially with distance, while the upstream wave is always damped. The exponential index, which gives the amplification, depends in a complicated way upon the wind velocity, the amount by which the wind velocity exceeds the velocity of propagation on the wire, the angle of attack, and the frequency of the disturbance.

Aerodynamic amplification of the type just described accounts very well for the observed failure of trailing-wire antennas. When the condition for high amplification exists a small mechanical motion introduced near the point of wire attachment, either by motion of the aircraft or by turbulence of the boundary layer air through which the antenna passes, will travel downstream on the wire, arriving at the end-weight as a large-amplitude wave. At the end-weight the wave is partially reflected giving a high amplitude standing wave. Moreover, coupling through wire curvature into longitudinal motion leads to tension variations in the wire. The violent motion existing near the point of weight attachment, combined with extreme tension variations, will quickly cause failure of the cable.

The vortex shedding responsible for instability of the first type described above can easily be eliminated by replacing the previously used sphere with a streamlined end-weight designed to possess inherent aerodynamic stability. Furthermore, the use of a heavy, very low-drag end-weight results in the electrically highly favorable cable configuration in which there is a region of appreciable length just above the end-weight where the wire departs only slightly from the vertical. The use of stabilizing fins does, however, give rise to still another form of system instability which occurs because of coupling between a weather-vane type of motion of the streamlined end-weight, and a lateral pendulum oscillation.[7] On the other hand, the spatial region in which this type of instability is possible is so close to the aircraft that the weight will never normally be in it except when passing into or out of the aircraft. Furthermore, the rate of growth of such oscillations is so small that they cannot attain significant amplitudes in the time the weight spends in the critical region.

Eliminating the second type of instability, that due to aerodynamic amplification, is much more difficult. Since this form of amplification occurs only when the component of wind velocity tangential to the wire exceeds the velocity of wave propagation along it, our first thought is to see whether the propagation velocity cannot be increased to a value greater than the wind velocity, even at very high speeds.

To a first approximation we can say that the propagation velocity of waves on the wire is the same as that which would obtain in a vacuum. It can be shown that this velocity, U_0, is given by

$$U_0 = \sqrt{\frac{\text{stress}}{\text{density}}} \ .$$

Hard-drawn steel wire has the highest available ratio of ultimate strength to density and for such wire stressed to the yield point the propagation velocity of the wave on the wire is approximately Mach 2. Since in any actual installation we must allow a substantial factor of safety, the highest propagation velocity that can be obtained in practical antennas will be of the order of Mach 1. If the airspeed exceeds this figure, the amplification can be reduced to unity only by increasing the weight of the terminating body to such a value that the entire cable is nearly vertical. For aircraft in the Mach 2 to Mach 3 speed range, it can be shown that the weights theoretically required would be of the order of 10 or 20 tons, and the cables would have to be of the order of ¼ to 1 inch in diameter. We therefore conclude that it is impossible practically to avoid having some amplification when the trailing wire is mounted on such aircraft. Attention, then, must be directed toward keeping this amplification within tolerable limits.

It is worthy of note that the amplification can also theoretically be reduced to a very low value by using a light end-weight of very high drag, so that the cable streams out almost horizontally. In practice, however, this design places the entire cable in the turbulent boundary layer and wake of the air vehicle, where the airflow is certainly not laminar and parallel to the cable at all points. This condition, which may very well result in extremely high amplification, will not be considered in this report.

Phillips' first order theory applies only to straight cables in uniform airstreams, and takes no account of the true shape of the antenna. The actual curved shape results in substantial departures from first-order predictions, particularly at lower frequencies. Furthermore, Phillips' theory assumes constant wire tension. Consequently it not only cannot predict the conditions under which failure occurs, but provides no insight into the circumstances under which the theory ceases to be approximately valid.

Since the preceding discussion makes it clear that aerodynamic wave amplification cannot possibly be avoided at speeds significantly above Mach 1, it is important to have a theory which more accurately describes the behavior of trailing wires at velocities where amplification can occur. To be useful the theory should include at least a first order description of the tension variations which can occur because of aerodynamic wave

amplification, since it is obvious that wire failure cannot take place without tension fluctuations. It should also show the effect of the curved shape of the wire upon the amplification and resultant wire tension. In this report such a theory is developed and applied to an experimental installation designed for flight testing under Air Force Contract AF 33(616)-5549. While the flight tests, because of limitations of the F-100 test vehicle, have been conducted at rather low supersonic speeds (up to Mach 1.24), the installation is designed to simulate the conditions of wave amplification likely to be encountered at the Mach 2 to Mach 3 speeds representative of the next generation of aircraft.

II ONE-DIMENSIONAL APPROXIMATION FOR WAVE AMPLIFICATION

A. PRELIMINARY CONSIDERATIONS

Before investigating the dynamic situation in which wave motion exists on the trailing wire it is necessary to explore the static condition, where the wire is in equilibrium under the action of the aerodynamic forces of the airstream and gravitational forces—principally those due to the end-weight. The shape of a trailing wire in an airstream has been considered by earlier investigators.[8,9] It is re-examined here, however, because it is possible to derive the results somewhat more succinctly than has been done heretofore, and in a form more suited to the analysis of the dynamic condition which follows.

B. DIMENSIONLESS EXPRESSIONS FOR EQUILIBRIUM WIRE SHAPE

The aerodynamic force on an element of cable suspended in a supersonic airstream is always nearly normal to the axis* of the element, and can be considered to arise entirely from the component of air velocity in the normal direction, V_n.[10] For cases of practical interest, the weight of the element can be neglected, and in the absence of mechanical waves on the cable the element is in equilibrium under the action of the aerodynamic force and the tensions at its ends (see Fig. 1). The tensions are equal in the static case because of the absence of any other tangential components of force—*i.e.*, $dT = 0$.

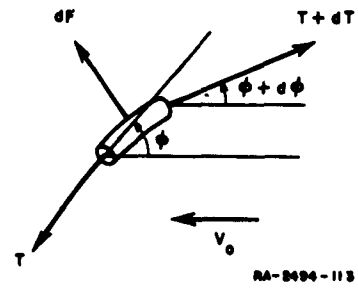

FIG. 1
FORCES ON AN ELEMENT OF WIRE

Let the following quantities be defined:

T = tension in cable

* The small component of aerodynamic force tangential to the cable element has been neglected, as its consideration would have made the solution of an already very complex problem even more involved. The principal effect of this force is to cause a variation in the static tension along the cable. Significant departures from the value predicted by the simpler theory occur, however, only in the upper part of long wires. In this region the effect of increased tension on cable shape is slight. A second effect of the increased tension—a decrease in aerodynamic amplification—is also quite small.

ds = length of element

ϕ = angle element makes with horizontal

V_0 = air velocity (horizontal).

Then, from Fig. 1 one can write for the mechanical force acting on the wire element

$$dF = -T\, d\phi \quad . \tag{1}$$

The aerodynamic force on the element is

$$dF = C_D \frac{\rho V_n^2}{2} (D\, ds) = C_D D \frac{\rho V_0^2}{2} \sin^2 \phi\, ds \tag{2}$$

where

C_D = drag coefficient of a cylinder

D = diameter of cable

ρ = air density.

For equilibrium the mechanical force equals the aerodynamic force, so that

$$-T\, d\phi = C_D D \frac{\rho V_0^2}{2} \sin^2 \phi\, ds \tag{3}$$

or

$$\frac{ds}{C} = -\csc^2 \phi\, d\phi \tag{4}$$

where C is a characteristic length given by

$$C = \frac{T}{C_D D \left(\frac{\rho V_0^2}{2}\right)} \quad . \tag{5}$$

Provided that the drag coefficient C_D can be considered constant along the cable,* Eq. (4) may easily be integrated to give

* See Sec. IV-A for a discussion of the importance of this limitation.

$$\cot \phi = \cot \Phi + \sigma \qquad (6)$$

as the equation of the cable shape, where σ is defined as the dimensionless arc length s/C. Although not apparent when written in this form, Eq. (6) is the equation of a catenary.

The slope angle of the lower end of the cable, Φ, is determined by the way in which the cable is terminated at that point. If the termination is provided by a body of very high weight-to-drag ratio the lower end of the wire will be essentially vertical, and the tension will be equal to the weight of the terminating body. If, in addition, the lower end is taken as origin of dimensionless Cartesian coordinates ξ and η, defined as x/C and y/C respectively, the following expressions result:

$$\xi = \int_{\phi'=\pi/2}^{\phi} d\sigma' \cos \phi' = \csc \phi - 1 \qquad (7)$$

$$\eta = \int_{\phi'=\pi/2}^{\phi} d\sigma' \sin \phi' = \ln (\csc \phi + \cot \phi) \quad . \qquad (8)$$

The four quantities ξ, η, σ, and ϕ can be expressed in terms of each other by means of various substitutions among the above equations. Complete results appear in Appendix A, and curves of the wire shape are shown in Fig. 2.

C. WAVE AMPLIFICATION IN A STRAIGHT WIRE

According to Phillips' theory, which is restricted to vibrations taking place in the plane determined by the air velocity and the wire direction, the amplification depends on the angle between wind and wire, and on the ratio of wave velocity to wind velocity. To the first order, the only effect of the wind on in-plane waves (for sufficiently high frequencies) is to cause the wave amplitude to vary exponentially along the wire. For a wave traveling downwind (negative-s direction along the wire in Fig. 2), the transverse displacement for a sinusoidal input is given by

$$n = a_0 \epsilon^{-ks} \epsilon^{i\omega(t+s/U)} \qquad (9)$$

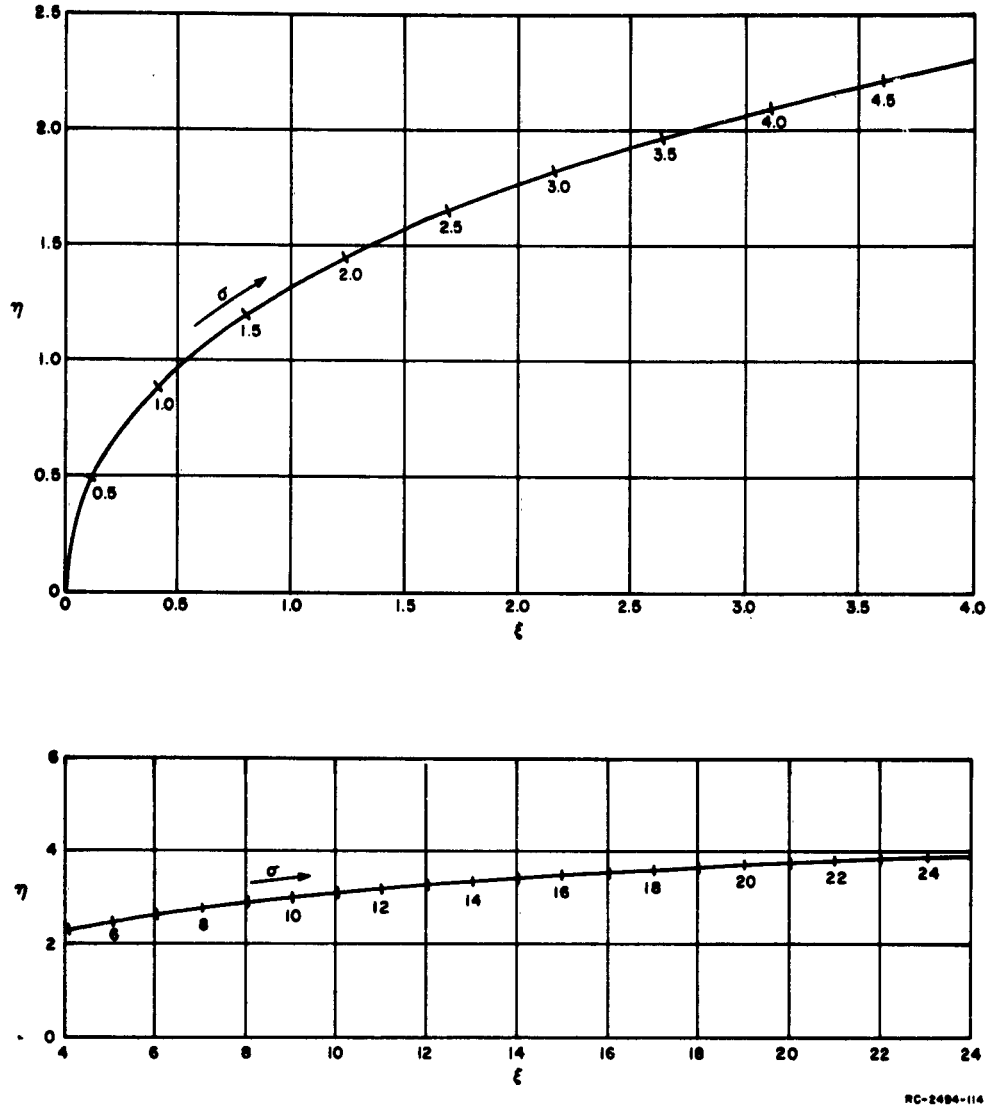

FIG. 2
SHAPE OF TRAILING WIRE

where U is the wave velocity on the wire, a_0 is a constant, and

$$k = \frac{1}{2C}\left(1 - \frac{U}{V_0 \cos \phi}\right) \sin 2\phi \quad . \tag{10}$$

It is seen that a wave traveling in the negative-s direction will be amplified if the component of wind velocity along the direction of the wire is greater than the wave velocity (k positive), and damped if it is less (k negative). For a wave traveling upwind, only the sign of U is changed in Eqs. (9) and (10). In this case, k is always positive and, since the wave travels in the positive-s direction, damping always occurs.

The above equation indicates that there can be no amplification when the wire is exactly parallel to the wind direction. Likewise, the theory predicts that no amplification will occur for vibrations taking place in a direction normal to the plane containing the cable. Actually this result stems from the neglect of certain terms in the first order theory. A more accurate investigation of wire behavior for zero angle of attack (see Appendix B) shows that there is a very small aerodynamic amplification for a downwind wave and very small damping for an upwind wave, in the case where one or the other exists on the wire alone.

When complete reflection of the lateral wave occurs at the lower end of the cable, the resulting standing wave consists of a combination of the two traveling waves, but the net damping cannot be computed by means of linear superposition. An approximate treatment of the aerodynamic damping is still possible, however, and shows that, in the absence of other damping mechanisms, the wire behaves as a very high-Q system with resonances at multiples of one-half wavelength.

The most extreme response occurs at one-half-wave resonance, where it is found that the standing wave amplitude is proportional to the square root of the input amplitude at the upper end of the cable. The theory developed in Appendix B takes no account of wire curvature or of other mechanisms providing coupling to the in-plane vibrations, which are of much lower Q. Moreover, the end-weight does not constitute a perfectly rigid termination, and therefore will furnish some damping due to its lateral drag.

The actual Q of the lateral vibrations will therefore be considerably lower than that predicted by Appendix B. For this reason, and more

importantly because first-order coupling to tension variations occurs only via the in-plane motion, it is not felt that the lateral motion is a significant cause of cable failure. The analysis given in the main body of this report will therefore be confined to vibrations in the plane of the wire.

D. TOTAL AMPLIFICATION IN THE CURVED WIRE

Equation (9) may be regarded as an equation for a, the wave amplitude along the wire, which may in the general case be complex:

$$a = a_0 \epsilon^{-ks} \quad . \tag{11}$$

The change in amplitude in an element of the wire is

$$da = -k\, a_0\, \epsilon^{-ks}\, ds = -a\, (\cos\phi - \gamma)\, \sin\phi\, d\sigma \tag{12}$$

where

$$\gamma = \frac{U}{V_0} \quad . \tag{13}$$

An approximation to the total amplification in a curved wire can be obtained by taking Eq. (12) as the differential equation for the amplitude, and inserting the known relation between σ and ϕ for the equilibrium shape of the wire. This is equivalent to the assumption that the transverse wave in the wire travels along the curve as if the wire were straight, remaining always transverse, but that the amplification coefficient varies in the correct fashion from point to point.

Since $d\sigma = \cot^2\phi\, d\phi$, we have

$$a^{-1}\, da = (\cos\phi - \gamma)\, \csc\phi\, d\phi \quad . \tag{12'}$$

If the amplitude at the origin (lower end of the cable) is taken to be a_0, and U (or γ) is assumed to be independent of ϕ, Eq. (12') leads to

$$a = a_0\, (\csc\phi + \cot\phi)^{\gamma}\, \sin\phi \tag{14a}$$

or

$$a = a_0 \left[\sigma + \sqrt{1 + \sigma^2}\right]^{\gamma} (1 + \sigma^2)^{-\frac{1}{2}} \quad . \tag{14b}$$

The amplification from a point σ on the wire down to the end is

$$A(0,\sigma) = \frac{a_0}{a(\sigma)} = (1+\sigma^2)^{1/2}\left[\sigma + \sqrt{1+\sigma^2}\right]^{-\gamma} \qquad (15)$$

while the amplification from a point σ_2 down to a lower point σ_1 is

$$A(\sigma_1,\sigma_2) = \frac{a(\sigma_1)}{a(\sigma_2)} = \frac{A(0,\sigma_2)}{A(0,\sigma_1)} \quad . \qquad (16)$$

E. THE REFLECTED WAVE

In general there will also be an upwind, or reflected, wave. The attenuation experienced by such a wave traveling from the origin to a point σ can be found from Eq. (15), using a negative value of γ. Loci of constant $A(0,\sigma)$ in the γ,σ plane are shown in Fig. 3. For example, if

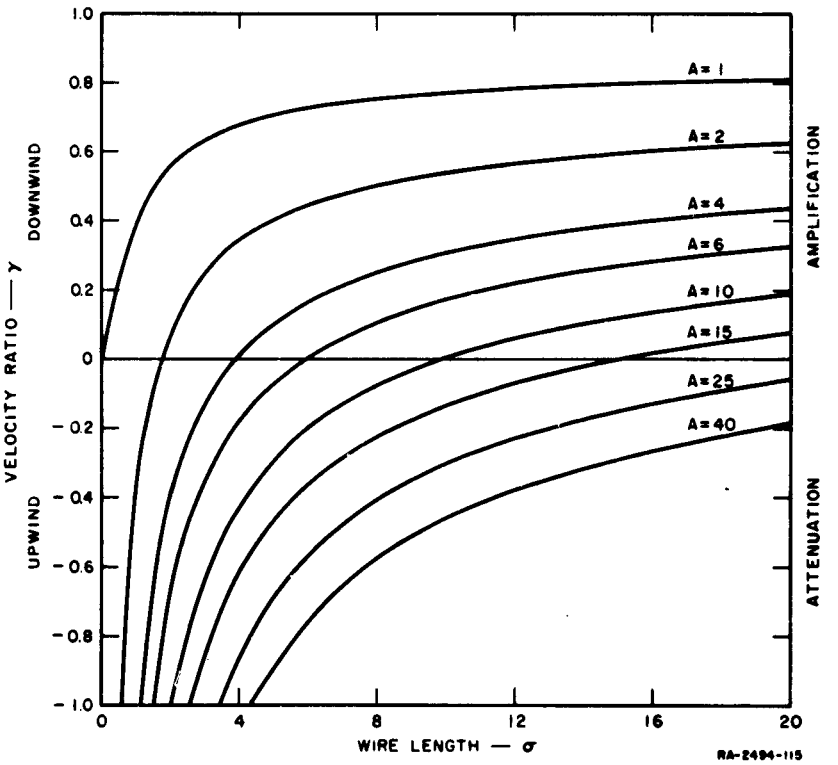

FIG. 3

AERODYNAMIC AMPLIFICATION CHARACTERISTICS OF TRAILING WIRE

the wind velocity is twice the wave velocity in the wire ($\gamma = 0.5$), the incident wave will be amplified by a factor of 2.3 in proceeding from $\sigma = 10$ to the end of the wire, while the reflected wave will be attenuated by a factor of 45 in returning to the same point. In using Fig. 3 it should be remembered that $\gamma = 0$ corresponds either to zero wave velocity or to infinite wind velocity.

F. THE COMPLETE SOLUTION

The complete solution for the transverse displacement on the cable for the case of a single sinusoidal excitation is, in the one-dimensional approximation of this chapter,

$$n = \frac{a_1}{A_1(0,\sigma)} \epsilon^{i\omega(t+C\sigma/U)} + \frac{a_2}{A_2(0,\sigma)} \epsilon^{i\omega(t-C\sigma/U)} \quad . \qquad (17)$$

The constants a_1 and a_2 represent the (complex) amplitudes of the incident and reflected waves respectively, at the origin. In a given case, they can only be evaluated through a knowledge of the appropriate boundary conditions—on the one hand the way in which the wire is terminated at its lower end, on the other the location of the input excitation and the phase relationship between the two waves at that same point.

For example, if no transverse motion of the lower end of the wire is permitted, then $a_2 = -a_1$—*i.e.*, complete reflection with phase reversal occurs. If the input, of amplitude n_Σ, is applied at the point $\sigma = \Sigma$, that is, if $n(\Sigma) = n_\Sigma \epsilon^{i\omega t}$, a_1 can be evaluated as follows:

$$a_1 = n_\Sigma [A_1^{-1} \epsilon^{i\omega C\Sigma/U} - A_2^{-1} \epsilon^{-i\omega C\Sigma/U}]^{-1} \quad . \qquad (18)$$

With the appropriate substitutions, Eq. (18) can be rewritten as

$$a_1 = \frac{1}{2} n_\Sigma \sqrt{1+\Sigma^2}\, \operatorname{csch}\left(\gamma \sinh^{-1}\Sigma + \frac{i\omega C\Sigma}{U}\right) \quad . \qquad (19)$$

The maximum response for excitation at a given point occurs if the frequency is such that that point is a node in the standing wave—*i.e.*, the distance from the end of the wire is an even number of quarter wavelengths. If this distance is an odd number of quarter wavelengths,

corresponding to excitation at an antinode, the response is minimum. Needless to say, since the reflected wave is attenuated in any given length of wire more than the incident wave is amplified in the same length, the two waves can never cancel each other at more than one point, in this case the origin. This fact tends to reduce the magnitude of the resonances. These may, however, be quite pronounced for small σ (short wires) at relatively high frequencies or for very small γ (very high airspeed) at any frequency.

The foregoing analysis is not entirely satisfactory for several reasons. First, the effect of wire shape on waves whose wavelengths are comparable with the radius of curvature has not been taken into account in any way. Second, the possibility of longitudinal motion of the wire, arising from the curvature, is not considered. Third, non-linear effects of various kinds are entirely ignored.

G. NON-LINEAR EFFECTS

The non-linear effects mentioned above come into play when wave amplitudes on the wire are not entirely negligible in comparison with wavelength. One such effect arises from the deviation of the sine function from the tangent function, by means of which it is approximated in the first-order theory.

A second effect, which may have a more profound influence on the behavior of the wire, is the variation in over-all length caused by the presence of a standing wave. Note that the total wave on the wire is a combination of a standing and a traveling wave—almost completely standing at the lower end for a rigid termination there, and predominantly traveling at the upper end in most cases of physical interest.

The longitudinal motion at the lower end produced in this way will give rise to tension fluctuations if it is necessary to accelerate a relatively large mass. It should be noted also that these fluctuations will take place at double the wave frequency. If their amplitude is greater than T, the cable tension, the cable will go slack during a portion of the cycle, then go taut again quite suddenly. In an extreme case the cable is slack most of the time and has very high tension for an extremely short interval. This condition is obviously one possible cause of cable failure.

It is shown in Appendix C that the amplitude of the length variation produced by a sinusoidal input on a wire of length Σ_0, when the incident

wave has amplitude a_1 at the lower end of the wire and is completely reflected there, is given approximately by the following equation.

$$\Sigma' = 2(\pi|a_1|/\lambda)^2 \tan^{-1} \Sigma_0 \cdot \qquad \text{(C-11)}$$

In the above equation a_1 and λ, the wavelength on the wire, must be specified in terms of the same units, and Σ' is then given in the usual dimensionless units of this theory. Eq. (C-11) holds closely only for wavelengths short compared with the radius of curvature of the wire.

It is not difficult to show that, if the input consists of several sinusoids having frequencies ω_n, phase angles ψ_n, and amplitudes a_{1n} at $\sigma = 0$, the length variation may be expressed by

$$\Delta\Sigma = \sum \Sigma'_n \cos(2\omega_n t + 2\psi_n) = \frac{\tan^{-1} \Sigma_0}{2} \sum \frac{\omega_n^2 a_{1n}^2}{U^2} \cos(2\omega_n t + 2\psi_n) \cdot \qquad (20)$$

An extension of Eq. (20) leads to the interesting corollary that the frequency spectrum of the input must have delta-function type singularities in order that there be any effect. A "white" input produces no variation in length. This fact is a result of the dependence of Eq. (20) upon the squares of the a_{1n}. In the limit of a continuous spectrum, the right hand side can be shown to approach zero.

It should be noted that there are other causes for tension variations, in particular the creation of a longitudinal wave as the transverse wave travels down the wire. This is a first-order effect, however, and it will be taken into account in the later sections of this report.

III EXACT DESCRIPTION OF THE WIRE MOTION— FIRST-ORDER THEORY

A. COORDINATE SYSTEM

The preceding chapter has given an approximate theory of transverse wave motion on the trailing wire, based on the assumptions that there is no longitudinal motion and that the tension in the wire does not vary with time. A more complete theory, including these effects, will now be given.

The position of a point on the cable will be described in terms of the Cartesian coordinates of its equilibrium position, x_0 and y_0, and its displacements from equilibrium in directions normal and tangential to the cable at that point, n and p respectively (See Fig. 4). The ordinary cartesian coordinates of the point are related as follows to those just described:

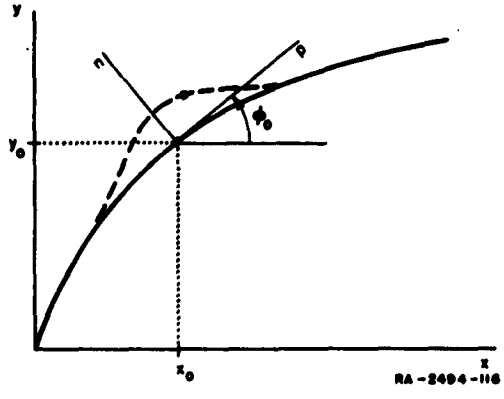

FIG. 4
COORDINATES OF A POINT ON THE WIRE

$$x = x_0 + p \cos \phi_0 - n \sin \phi_0 \qquad (21a)$$

$$y = y_0 + p \sin \phi_0 + n \cos \phi_0 \ . \qquad (21b)$$

B. EQUATIONS OF MOTION

An element of the wire in vibration is acted upon as before by the forces shown in Fig. 1. Now, however, the forces and angles may be functions of time and dT is no longer identically zero. The component of air velocity normal to the element of wire is given by

$$V_n = V_0 \sin \phi - \frac{\partial n}{\partial t} \tag{22}$$

where ϕ is the actual (displaced) direction of the element. If $\partial n/\partial t << V_0 \sin \phi_0$, then from Eq. (2) one can write for the aerodynamic force

$$dF = C_D \frac{\rho V_0^2}{2} D\, ds \sin^2 \phi \left(1 - \frac{2}{V_0} \frac{\partial n}{\partial t} \csc \phi\right) . \tag{23}$$

From Fig. 1 it can be seen that

$$dF + T \frac{\partial \phi}{\partial s} ds = \mu ds \frac{\partial^2 n}{\partial t^2} \tag{24}$$

where μ represents the cable mass per unit length. Now let $T = T_0 (1 + \beta)$, where T_0 is the average tension, and β is a function of position and time, assumed small compared to unity for the purposes of this theory. Let $U_0 = \sqrt{T_0/\mu}$ represent the ordinary wave velocity corresponding to the average tension. In addition, the following new dimensionless quantities are defined:

$$N = \frac{n}{C}$$

$$P = \frac{p}{C}$$

$$\tau = \frac{U_0 t}{C} .$$

The quantities C, ξ, η, σ, and γ are defined as in Sec. II of this report.

Eq. (24) now becomes

$$\left(1 - 2\gamma \frac{\partial N}{\partial \tau} \csc \phi\right) \sin^2 \phi + (1 + \beta) \frac{\partial \phi}{\partial \sigma} = \frac{\partial^2 N}{\partial \tau^2} . \tag{25}$$

For the static case $\partial^2 N/\partial\tau^2$, $\partial N/\partial\tau$, and β are all equal to zero, and Eq. (25) gives the static shape of the cable: $\sin^2 \phi_0 + \partial\phi_0/\partial\sigma = 0$, and $\sigma = \cot \phi_0$, as before. It is desirable to expand ϕ about ϕ_0 as follows:

$$\phi(\sigma,\tau) = \phi_0(\sigma) + \alpha(\sigma,\tau) \quad . \tag{26}$$

It is possible to show, by means of Eqs. (21a), (21b), and (26), and elementary trigonometry, that

$$\alpha = \frac{\partial N}{\partial\sigma} + P \frac{\partial\phi_0}{\partial\sigma} \quad . \tag{27}$$

With $\alpha \ll 1$,

$$\sin^2 \phi = \sin^2 \phi_0 + 2\alpha \sin \phi_0 \cos \phi_0 \tag{28a}$$

$$\csc \phi = \csc \phi_0 - \alpha \csc \phi_0 \cot \phi_0 \quad . \tag{28b}$$

Eqs. (26), (27), (28a) and (28b) may now be substituted into (25), α and β being treated as small quantities whose products and squares are neglected. Using the known equilibrium shape of the wire, and remembering from Eq. (22) that $\gamma\ (\partial N/\partial\tau) \ll \sin \phi$, one obtains finally the following differential equation of motion normal to the cable:

$$\frac{\partial^2 N}{\partial\sigma^2} + \frac{2\sigma}{1+\sigma^2}\frac{\partial N}{\partial\sigma} - \frac{1}{1+\sigma^2}\frac{\partial P}{\partial\sigma} - \frac{1}{1+\sigma^2}\beta = \frac{\partial^2 N}{\partial\tau^2} + 2\gamma \frac{1}{(1+\sigma^2)^{1/2}}\frac{\partial N}{\partial\tau} \quad . \tag{29}$$

A second examination of Fig. 1 leads to the following:

$$\frac{\partial T}{\partial s} ds = \mu ds \frac{\partial^2 p}{\partial t^2} \tag{30}$$

or

$$\frac{\partial\beta}{\partial\sigma} = \frac{\partial^2 P}{\partial\tau^2} \quad . \tag{31}$$

This is the differential equation for motion tangential to the cable.

C. INEXTENSIBILITY OF THE CABLE

Eqs. (29) and (31) give two relations among the three variable N, P, and β. The problem is therefore not yet sufficiently determined for a solution. A third relation may be obtained from the elastic properties of the cable. If, as before, the cable is considered to be inextensible, one must have

$$ds^2 = dx^2 + dy^2 = dx_0^2 + dy_0^2 \quad . \tag{32}$$

With the help of Eq. (21a,b), and remembering that n and p are small compared with x_0 and y_0, one easily obtains

$$n \frac{\partial \phi_0}{\partial s} = \frac{\partial p}{\partial s} \tag{33}$$

or

$$N = -(1 + \sigma^2) \frac{\partial P}{\partial \sigma} \quad . \tag{34}$$

Eq. (34), together with Eqs. (29) and (31), yields in principle a complete solution to the problem, provided the appropriate boundary conditions are specified.

D. SIMULTANEOUS SOLUTION OF PARTIAL DIFFERENTIAL EQUATIONS

It is possible to eliminate either P and β or N and β from the system of three partial differential equations. The result in either instance is a fourth-order linear partial differential equation whose coefficients are rather complicated functions of σ.

Because the coefficients are independent of time, it is possible to find product solutions in which the time occurs only through the factor $\epsilon^{i\nu\tau}$—*i.e.*, let

$$N(\sigma,\tau) = u(\sigma)\epsilon^{i\nu\tau} \tag{35a}$$

$$P(\sigma,\tau) = v(\sigma)\epsilon^{i\nu\tau} \tag{35b}$$

$$\beta(\sigma,\tau) = r(\sigma)\epsilon^{i\nu\tau} \quad . \tag{35c}$$

Such solutions represent the steady-state behavior of the wire under the influence of a single sinusoidal excitation of dimensionless frequency ν, defined as follows:

$$\nu = \frac{C}{U_0}\omega \tag{36}$$

where ω is the angular frequency of the input.

Formal substitution of Eq. (35a) or Eq. (35b) into one of the above-mentioned fourth-order equations converts it into a linear, fourth-order, ordinary differential equation with complex, non-constant coefficients.

In principle it is then possible to obtain the functions $w(\sigma)$, $v(\sigma)$, $r(\sigma)$ in a particular case, provided four suitable boundary conditions are supplied. In practice, however, the nature of the differential equations is such that it is nearly impossible to obtain any sort of general information from them. In fact, any attempt to find approximate forms of a literal solution becomes rapidly so involved as to obscure entirely the basic phenomena which it is desired to represent.

E. THE UNIFORM-TENSION CASE

In many cases of physical interest, the total mass of the wire is very much smaller than that of the end-weight. Under these circumstances, the fluctuation in tension produced at the lower end of the wire by acceleration of the end-weight is much larger than any variation with distance along the wire produced by longitudinal acceleration of the wire itself. This is especially true for long (large Σ) wires where the inputs are largely transverse, as then any longitudinal motion is confined almost entirely to the lower part of the wire, between $\sigma = 0$ and $\sigma \approx 2$.

If the conditions described above are satisfied, the tension can be considered to be independent of σ, although the time dependence remains. In other words, the tension variation amplitude $r(\sigma)$ becomes a (complex) constant, whose value is determined by the boundary conditions at $\sigma = 0$. Eqs. (34), (35a), and (35c) may now be substituted into Eq. (29), giving

$$w'' + \frac{2\sigma}{1+\sigma^2}\,w' + \left[\frac{1}{(1+\sigma^2)^2} + \nu^2 - 2i\gamma\nu\,\frac{1}{(1+\sigma^2)^{1/2}}\right] w = \frac{1}{1+\sigma^2}\,r \tag{37}$$

where primes denote differentiation with respect to σ.

A further simplification may be effected through the following substitution:

$$w(\sigma) = (1 + \sigma^2)^{-\frac{1}{2}} u(\sigma) \quad . \tag{38}$$

The result is

$$u'' + \nu^2 f(\sigma)\, u = (1 + \sigma^2)^{-\frac{1}{2}} r \quad , \tag{39}$$

where

$$f(\sigma) = 1 - 2i(\gamma/\nu)(1 + \sigma^2)^{-\frac{1}{2}} \quad . \tag{40}$$

The general solution of Eq. (39) will consist of a homogenecus solution containing two arbitrary constants, plus a particular integral which will be proportional to r.

If $f(\sigma)$ is sufficiently slowly-varying, a very good approximation to the homogeneous solutions is given by

$$u = \text{const} \times \exp[\pm i\, \nu \int \sqrt{f(\sigma)}\, d\sigma] \quad . \tag{41}$$

For the range of values of γ and ν represented by the shaded portion of Fig. 5 (Regions I and II), the approximation of Eq. (41) holds, and it is possible to obtain analytic solutions of the following form:

$$u_1(\sigma) = (\sigma + \sqrt{1 + \sigma^2})^{\gamma} \exp\{i\, \nu\, [\sigma + (1/2)(\gamma/\nu)^2 \tan^{-1} \sigma]\} \tag{D-14a}$$

$$u_2(\sigma) = (\sigma + \sqrt{1 + \sigma^2})^{-\gamma} \exp\{-i\, \nu\, [\sigma + (1/2)(\gamma/\nu)^2 \tan^{-1} \sigma]\} \quad . \tag{D-14b}$$

Details of the derivation of (D-14a,b) and the determination of the boundaries in Fig. 5 may be found in Appendix D.

The arc-tangent term represents a deviation of the wave velocity from its normal value U_0 which is not sufficient to alter the amplification in this order of approximation. This term can be ignored in Region I of Fig. 5, but even in Region II, where strictly speaking it cannot, only the phase of the wave at points other than the origin is affected.

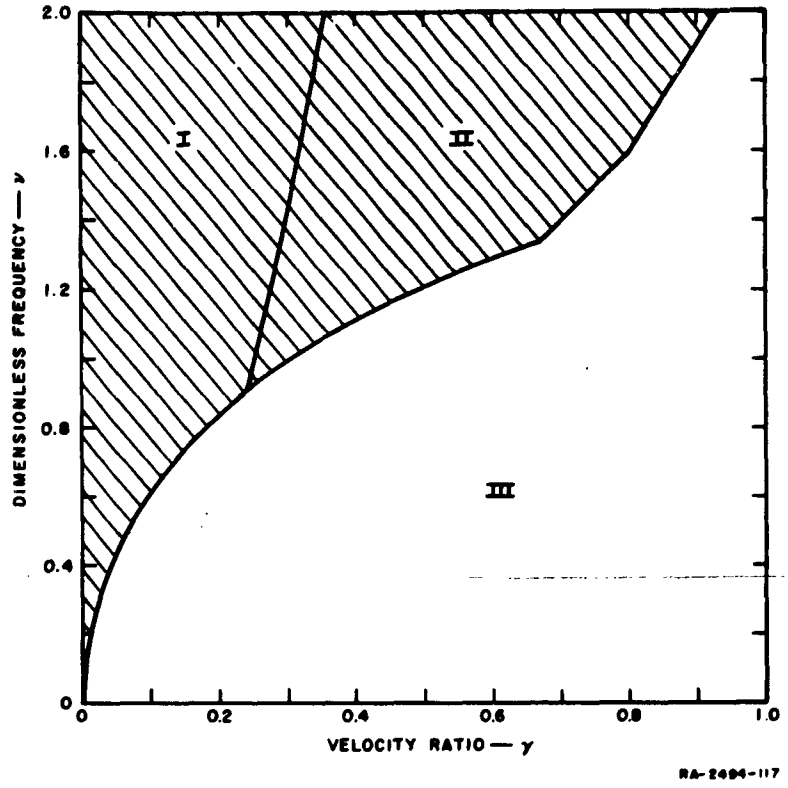

FIG. 5
DOMAINS OF VALIDITY OF SOLUTIONS

For the sake of mathematical simplicity, the remainder of this investigation will be limited to the case where this term is neglected, with the understanding that it could be included if necessary. Using Eqs. (35a) and (38), one then has

$$N_1(\sigma,\tau) = (1+\sigma^2)^{-1/2}\,(\sigma+\sqrt{1+\sigma^2})^{\gamma}\,\epsilon^{i\nu(\tau+\sigma)} \qquad (42a)$$

$$N_2(\sigma,\tau) = (1+\sigma^2)^{-1/2}\,(\sigma+\sqrt{1+\sigma^2})^{-\gamma}\,\epsilon^{i\nu(\tau-\sigma)} \qquad (42b)$$

which are easily seen to be identical with the solutions for the transverse wave obtained by the simple approach of Sec. II of this report.

It will be remembered that the complete solution of Eq. (39) consists of the homogeneous solutions, Eqs. (D-14a,b) plus a particular integral. The latter may be represented as $r\, u_3(\sigma)$, where $u_3(\sigma)$ is a particular integral of the following equation:

$$u'' + \nu^2 f(\sigma)\, u = (1 + \sigma^2)^{-\frac{1}{2}} \quad . \tag{43}$$

There are several well-known and straightforward methods for finding an integral of such an equation. In this case, however, all require one or more numerical integrations for each value of ν which it is desired to consider. Also, since there is an infinite number of particular integrals differing by arbitrary multiples of the homogeneous solutions, there is no assurance that one of these methods will yield an integral which will aid in the physical interpretation of the problem.

If the range of σ which is of interest in a particular case is known, a suitable approximate expression for $(1 + \sigma^2)^{-\frac{1}{2}}$ may be found in a form which can be handled analytically. An expression in the form of a sum of exponentials is especially useful, as it leads to an integral which becomes very small for values of σ greater than a few times unity—*i.e.*, for the less sharply curved portions of the wire. In addition, for many cases the solution is very nearly pure real and positive, corresponding to a sort of heaving motion of the wire as a whole. (See Sec. IV for a specific application of this approach.)

Thus, one is led to a representation of the wire motion in terms of a downward-traveling wave u_1, a reflected, or upward-traveling, wave u_2, and a heaving motion u_3 which is most important in the lower, more sharply curved, portions of the wire. The general motion of the wire can be written as

$$N(\sigma,\tau) = (1 + \sigma^2)^{-\frac{1}{2}} [b_1 u_1(\sigma) + b_2 u_2(\sigma) + r\, u_3(\sigma)]\, \epsilon^{i\nu\tau} \tag{44}$$

where b_1 and b_2 are arbitrary constants yet to be determined and r is the complex amplitude of the fractional tension fluctuation in the wire.

The general longitudinal motion of the wire can be obtained from Eq. (44) by means of Eq. (34). The result is

$$P(\sigma,\tau) = [v(0) - b_1 v_1(\sigma) - b_2 v_2(\sigma) - r\, v_3(\sigma)]\, \epsilon^{i\nu\tau} \qquad (45)$$

where

$$v_n(\sigma) = \int_0^\sigma (1 + \sigma'^2)^{-3/2}\, u_n(\sigma')d\sigma' \quad . \qquad (46)$$

F. APPLICATION OF BOUNDARY CONDITIONS

It will be remembered that the exact solution of the problem revolves about a fourth-order linear differential equation. Since such an equation requires the specification of four boundary conditions, any approximate solution, to be valid, must contain the same number of conditions.

If the case of interest is that in which the input is at the upper end of the trailing wire, then the first two conditions will be the specification of $N(\Sigma,\tau)$ and $P(\Sigma,\tau)$, the transverse and longitudinal inputs at the upper end of the cable. The remaining two conditions will depend upon the manner of termination of the cable at its lower end. One will be a relation connecting $\beta(\tau)$, the tension fluctuation, with $P(0,\tau)$, the longitudinal response of the terminating body. The other will describe the transverse response of the same body by means of a relation between $\partial N/\partial\sigma(0,\tau)$ and $N(0,\tau)$. Now $N(\Sigma,\tau) = w(\Sigma)\epsilon^{i\nu\tau}$, and an application of Eq. (44) at $\sigma = \Sigma$ yields

$$(1 + \Sigma^2)^{1/2}\, w(\Sigma) = b_1 u_1(\Sigma) + b_2 u_2(\Sigma) + r\, u_3(\Sigma) \quad . \qquad (47)$$

Proceeding in the same manner with Eq. (45), one obtains

$$v(\Sigma) = v(0) - b_1 v_1(\Sigma) - b_2 v_2(\Sigma) - r\, v_3(\Sigma) \quad . \qquad (48)$$

The varying tension in the cable will, in general, produce a response of the terminating weight, which will depend upon the method of attachment, damping forces present, etc. This response can always be expressed by means of a complex coupling constant ζ_p, as follows:

$$v(0) = \zeta_p' r \quad . \qquad (49)$$

Similarly, there will be a transverse motion of the weight in response to the transverse component of the tension force applied to it:

$$w(0) = \zeta_N w'(0) \quad . \tag{50}$$

This is equivalent to the following:

$$b_1 + b_2 + r\, u_3(0) = (\gamma + i\nu)\zeta_N b_1 - (\gamma + i\nu)\zeta_N b_2 + \zeta_N\, r\, u_3'(0) \quad . \tag{51}$$

If Eq. (49) is substituted into Eq. (48), and Eqs. (47) and (51) are rewritten, one obtains the following system of algebraic equations:

$$\left.\begin{aligned} u_1(\Sigma)b_1 + u_2(\Sigma)b_2 + u_3(\Sigma)r &= (1+\Sigma^2)^{\frac{1}{2}}\, w(\Sigma) \\ v_1(\Sigma)b_1 + v_2(\Sigma)b_2 + [v_3(\Sigma) - \zeta_p]r &= -v(\Sigma) \\ [1 - (\gamma + i\nu)\zeta_N]b_1 + [1 + (\gamma + i\nu)\zeta_N]b_2 + [u_3(0) - \zeta_N u_3'(0)]r &= 0 \end{aligned}\right\} \tag{52}$$

Eqs. (52) can readily be solved for b_1, b_2, and r, if the four boundary conditions are expressed in terms of $w(\Sigma)$, $v(\Sigma)$, ζ_p, and ζ_N.

In addition to the vibrational inputs expected at the point of attachment to the airframe, there will be, depending upon speed and details of the mechanical configuration, other inputs at points farther down the wire resulting from the action of oblique shock waves originating on the airframe. Because of their lower point of application, the amplification will be less, but the net effect is difficult to assess theoretically in the absence of experimental data.

G. LOW FREQUENCY BEHAVIOR

It is of considerable interest to examine the behavior of low-frequency waves on the wire under conditions for which the approximations of the preceding theory do not hold (Region III of Fig. 5). It will be remembered that the approximate theory of Sec. II gives correct results for the transverse motion for the case where the end is longitudinally free—that is, where the longitudinal motion is ignored. More importantly, it gives the correct value for the amplification undergone by the

downward-traveling wave, which is the primary factor governing the amplitude of transverse motion near the lower end of the wire and the severity of the tension fluctuations if the end is restrained.

If the propagation of a wave in a straight piece of wire is considered, it is easily found that, for sufficiently high frequencies, the wave velocity is independent of frequency and of the angle made with the airstream, having a value of $\sqrt{T_0/\mu}$. However, for lower frequencies, the velocity depends on the angle and in general increases with decreasing frequency. The ratio of this velocity to the high frequency value (*cf.* W. H. Phillips[5]) is given by

$$\frac{U}{U_0} = \nu\sqrt{2}\left\{(\nu^2 - \sin^2\phi\cos^2\phi) + \left[(\nu^2 - \sin^2\phi\cos^2\phi)^2 + 4\gamma_0^2\nu^2\sin\phi\right]^{1/2}\right\}^{-1/2} . \tag{53}$$

This expression may be used to compute, for any given ν, a corrected value of γ. Then, ignoring the effect of wire curvature, Eq. (13) leads to

$$A_1(0,\Sigma) = \exp\left\{-\int_{\pi/2}^{\cot^{-1}\Sigma}[\cos\phi - \gamma(\phi,\nu)]\csc\phi\, d\phi\right\} . \tag{54}$$

This amplification is shown as a function of ν in Fig. 6 for a wire of $\Sigma = 10$ and the flight parameters of Sec. IV of this report—*i.e.*, for $\gamma_0 = 0.23$. The results can be interpreted to indicate, at least qualitatively, that the amplification decreases rapidly for very low frequencies.

However, it is also found that the attenuation of the reflected wave computed in this way decreases to unity at these low frequencies. As a result, there is little net aerodynamic damping in the path from the upper end of the cable to the lower and back again, and the resonances which occur for certain frequencies can therefore be very extreme unless there are other sources of mechanical damping.

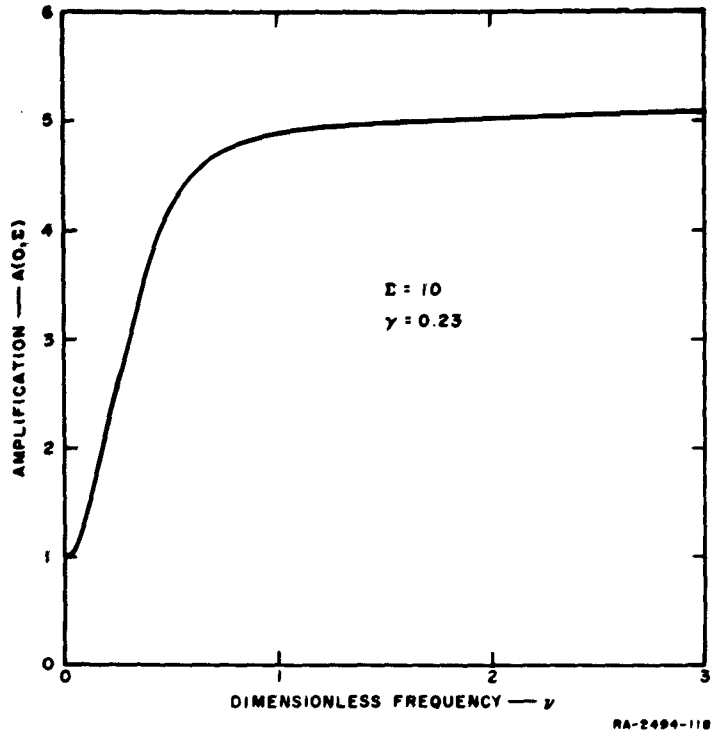

FIG. 6
INCIDENT WAVE AMPLIFICATION AT LOW FREQUENCIES

H. NON-AERODYNAMIC DAMPING

The analysis to this point has entirely neglected damping from sources other than the airstream itself. Such damping may arise through the action of viscous forces within the cable, or through the transfer of energy to another, coupled, mode of oscillation.

The first type of damping can be described in terms of a damping constant K characteristic of the particular cable used. The effect will be to decrease the amplification of the incident wave by a factor $\exp(-KC\Sigma)$, and to increase the damping of the reflected wave by the same factor. Qualitatively, the amplitudes near the lower end will be reduced for any set of conditions, while the resonant fluctuations of these amplitudes with cable length will become less pronounced because of the decrease in reflected wave amplitude at the input point (the upper end) relative to the incident wave.

The quantitative effect may perhaps most easily be seen by rewriting Eqs. (19) and (42a,b) to include this damping:

$$a_1 = \frac{1}{2}\, n_\Sigma \sqrt{1+\Sigma^2}\ \operatorname{csch}\left[\gamma \sinh^{-1}\Sigma + KC\Sigma + i\nu\Sigma\right] \qquad (19)$$

$$N_1(\sigma,\tau) = (1+\sigma^2)^{-\frac{1}{2}} \left(\sigma + \sqrt{1+\sigma^2}\right)^{\gamma} \epsilon^{KC\sigma} \cdot \epsilon^{i\nu(\tau+\sigma)} \qquad (42a)$$

$$N_2(\sigma,\tau) = (1+\sigma^2)^{-\frac{1}{2}} \left(\sigma + \sqrt{1+\sigma^2}\right)^{-\gamma} \epsilon^{-KC\sigma}\, \epsilon^{i\nu(\tau-\sigma)} \quad . \qquad (42b)$$

The most important case of the second type is the coupling which is certain to occur between the oscillations in the vertical plane and lateral oscillations perpendicular to that plane. As pointed out in Sec. II-B, the latter kind of motion experiences only slight aerodynamic amplification or damping.

Lateral vibrations will arise in two ways. First, there will be direct lateral inputs at the upper end of the wire and to a lesser extent along the wire. Second, there will be the coupled energy from the in-plane vibrations, as mentioned above. The total attenuation in a round trip to the lower end of the cable and back to the input point is actually less for these waves than the net attenuation for the in-plane waves. However, because there is no amplification of the incident waves, their contribution to the amplitude at the lower end will be small. Without detailed knowledge of the coupling mechanism it is most difficult to analyze this effect in a quantitative way, but qualitatively it can be seen that the total amplitudes on the lower parts of the wire will be reduced.

Both of the damping mechanisms described above will be more effective for a stranded cable, in the one case because of the obvious increase in internal friction, in the other because the helical form of individual wire strands tends to rotate the plane of vibration of the wire, converting an in-plane vibration to a lateral vibration.

IV APPLICATION OF THE THEORY TO A PARTICULAR PROBLEM

A. FLIGHT PARAMETERS AND CONSTANTS OF AN EXPERIMENTAL TRAILING-WIRE ANTENNA

Computations have been made for an experimental trailing-wire antenna whose mechanical properties have been tested in flight at about 35,000 feet altitude and speeds up to Mach 1.24. Results of these highly successful flight tests will be presented as a part of the final report on another SRI project.*

The cable, 1/16 inch in diameter, was tested at lengths up to 150 feet. It is terminated in a 19-pound fin-stabilized weight of high fineness ratio, attached at its center of gravity to the cable. Two systems of springing were investigated, one an essentially rigid coupling, the other a pre-stressed spring permitting approximately a ± 10-percent variation in cable tension with a ± 1-inch travel in the vertical direction. The drag on the end-weight in flight is quite small, so that the cable is essentially vertical at its lower end, and the static value of tension is very nearly equal to the weight, or 19 pounds.

The accepted value of the drag coefficient for a circular cylinder of infinite length, at moderate subsonic Mach numbers and subcritical Reynolds numbers, is 1.20.[11,12] As the Mach number is increased above 0.3, the coefficient rises with some irregular variations to a maximum of 2.13 just below sonic speed. Beyond this maximum, a decline occurs toward an asymptotic value of 1.33.[12] Clearly, the value of drag coefficient for a trailing-wire antenna will be a function of the speed of the aircraft, and also will vary with position along the cable. However, the physically interesting case of high wave amplification always implies large values of dimensionless cable length Σ, and therefore very small angles of attack over most of the length of the cable (see Fig. 2). As a result, even when the aircraft speed is highly supersonic the transverse airflow across most of the wire is subsonic. It is possible to compute both the cable shape and the total amplification exactly in a given case by means of numerical integration.

* SRI Project 2484, "Investigation of an Excited Airframe as an Antenna."

However, it has been found that a constant value of $C_D = 1.25$ gives the correct value of amplification within about 5 percent over a very wide range of flight conditions, and it has been adopted for the sake of computational simplicity. On this basis, and with the additional information that μ, the cable mass per unit length, is 2.34×10^{-4} slug/ft, one finds for Mach 1.24 at 35,000 feet altitude and a typical cable length of 100 feet.

$$\gamma = 0.23$$
$$C = 5.25 \text{ feet}$$
$$\Sigma = 19.0 \ .$$

The cable shape for these conditions, on the other hand, corresponds more nearly to $C_D = 1.44$.

The weight of the wire at this length is only 1.13 pounds, and therefore the uniform-tension approximation of Sec. III-E is justified. Reference to Fig. 5 shows that the system parameters lie in Region I, where the simplest form of solution holds if ν is greater than about 0.88, corresponding to an actual frequency of 7.6 cycles. The aerodynamic amplification of the downwind wave is 8.2.

The system described above is designed to simulate the aerodynamic amplification of a hypothetical higher-speed system identical to it in all respects except for the use of a 50-pound end-weight. On the basis of a 100-foot wire, the following are typical speed-altitude combinations for the hypothetical system which give the same theoretical amplification as the experimental system does in the Mach 1.24 flight test:

Mach 2.0 - 35,000 feet

Mach 2.5 - 48,500 feet

Mach 3.0 - 59,000 feet.

It should be noted that, although the wave amplification is the same in all the above cases, the cable shape differs from one case to another because each represents a different γ, Σ combination.

B. COMPUTATION OF THE $u_n(\sigma)$ AND $v_n(\sigma)$

The magnitudes of the two homogeneous solutions $u_1(\sigma)$ and $u_2(\sigma)$ (downwind and upwind waves, respectively) depend only upon γ, and have been shown in Fig. 7 for $\gamma = 0.23$. The phases, of course, depend upon position through the factors $\epsilon^{\pm i\nu\sigma}$.

The particular integral $u_3(\sigma)$ is a solution of Eq. (43), which is here repeated for convenience:

$$u'' + \nu^2 f(\sigma)\, u = (1 + \sigma^2)^{-1/2} \quad . \tag{43}$$

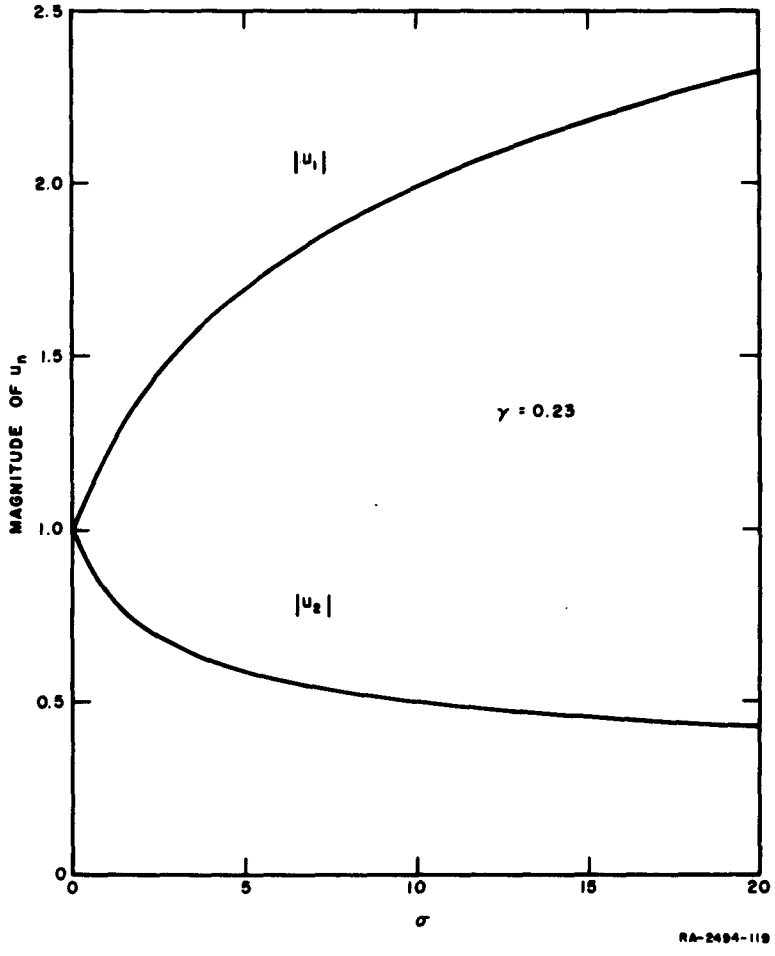

FIG. 7
MAGNITUDES OF TRAVELING WAVE SOLUTIONS

The solution, which is in general complex, will be written in the following form:

$$u_3(\sigma) = x(\sigma) + i\, 2\gamma\nu\, y(\sigma) \tag{55}$$

where $x(\sigma)$ and $y(\sigma)$ are real. If Eq. (55) is substituted into Eq. (43), and real and imaginary parts of the resulting equation are written separately, one obtains the following:

$$x'' + \nu^2 [x + 4\gamma^2 (1 + \sigma^2)^{-\frac{1}{2}}\, y] = (1 + \sigma^2)^{-\frac{1}{2}} , \tag{56a}$$

$$y'' + \nu^2\, y = (1 + \sigma^2)^{-\frac{1}{2}}\, x . \tag{56b}$$

This system of equations can be solved quite readily for x and y if

$$|4\gamma^2\, (1 + \sigma^2)^{-\frac{1}{2}}\, y| << |x| . \tag{57}$$

A procedure for finding a particular integral of Eqs. (56a,b) under the assumption that Eq. (57) holds is given in Appendix E. Resulting values of $u_3(\sigma)$ are shown in Figs. 8(a), (b) for the experimental system at several frequencies.

Detailed examination of a number of cases shows that at worst ($\nu \tilde{=} 1$, $\sigma = 0$) the left side of Eq. (57) is about 13 percent of the right side. Although this would seem to make the approximation rather marginal, both $|y|x|$ and $(1 + \sigma^2)^{-\frac{1}{2}}$ decrease rapidly with σ, and $|y/x|$ also decreases with ν. Thus the neglected term is nearly always much smaller than 13 percent of the leading term.

The longitudinal wave functions $v_n(\sigma)$ can readily be obtained from the $u_n(\sigma)$ through numerical evaluation of Eq. (46). The integral converges very rapidly to a constant value $v_n(\infty)$ for $\sigma \gtrsim 5$. These asymptotic values are shown in Table I.

TABLE I

ν	1	2	3	4	5
$v_1(\infty)$	0.851 $\angle$ 41.4°	0.586 $\angle$ 63.1°	0.414 $\angle$ 76.2°	0.305 $\angle$ 83.9°	0.234 $\angle$ 88.1°
$v_2(\infty)$	0.689 $\angle$ -34.8°	0.508 $\angle$ -55.4°	0.378 $\angle$ -68.6°	0.288 $\angle$ -76.9°	0.227 $\angle$ -82.0°
$v_3(\infty)$	0.652 $\angle$ 12.9°	0.1915 $\angle$ 9.1°	0.0874 $\angle$ 6.6°	0.0493 $\angle$ 5.1°	0.0315 $\angle$ 4.2°

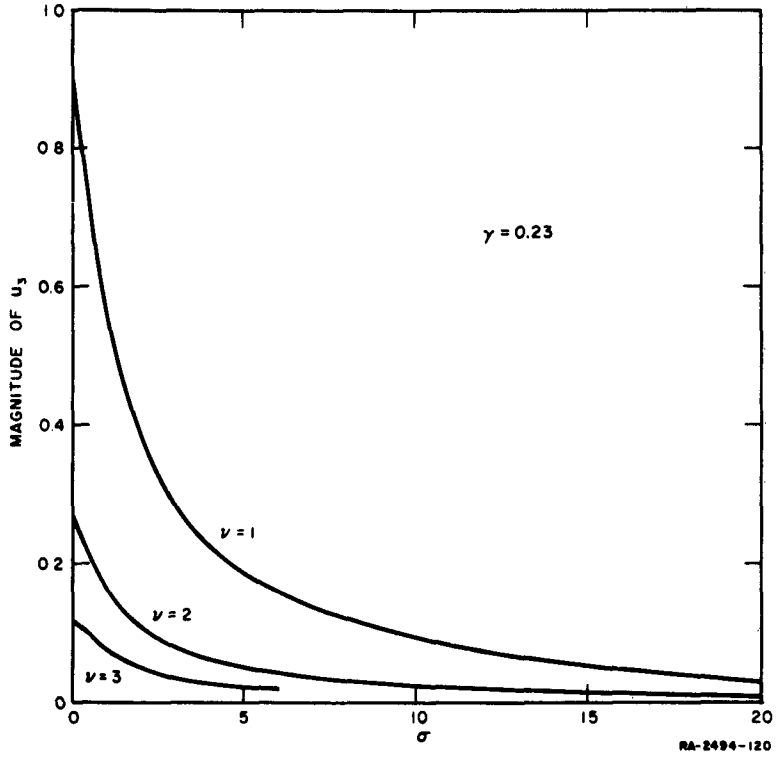

FIG. 8(a)
MAGNITUDE OF u_3

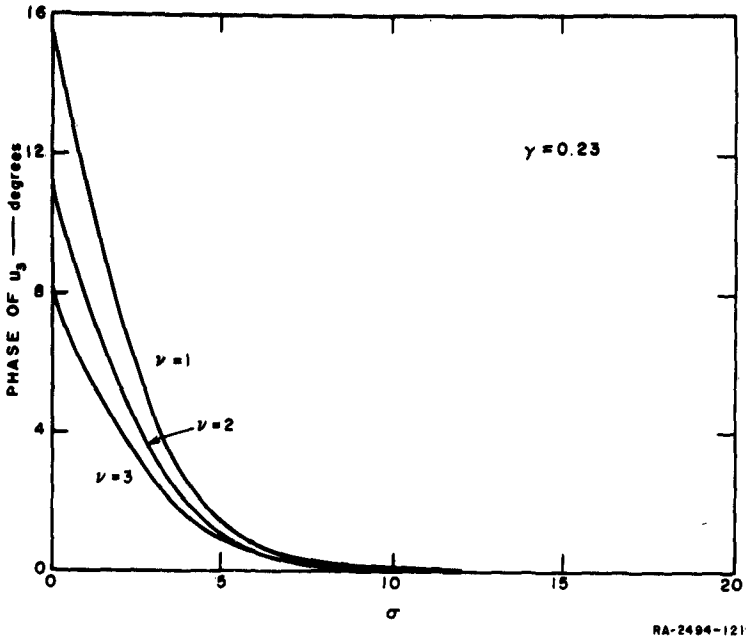

FIG. 8(b)
PHASE OF u_3

C. RIGID TERMINATION

If the lower end of the cable is attached directly to the center of mass of a heavy, stable end-weight, practically no motion of that point will take place. Mathematically, this condition is expressed as follows in terms of the two mechanical coupling coefficients:

$$\zeta_P = 0 \quad , \quad \zeta_N \neq 0 \quad . \tag{58a,b}$$

Let us suppose that the vibrational input at the upper end of the wire is purely transverse and of unit amplitude—*i.e.*,

$$v(\Sigma) = 0 \quad , \quad w(\Sigma) = 1 \angle 0^\circ \quad . \tag{59a,b}$$

Further let it be assumed that

$$\Sigma \gtrsim 5 \quad . \tag{60}$$

Then the amplitudes of the incident and reflected waves, as well as the resulting tension fluctuation, can be computed with the aid of Eqs. (52), which may now be written as follows:

$$\begin{pmatrix} u_1(\Sigma) & u_2(\Sigma) & u_3(\Sigma) \\ v_1(\infty) & v_2(\infty) & v_3(\infty) \\ 1 & 1 & u_3(0) \end{pmatrix} \begin{pmatrix} b_1 \\ b_2 \\ r \end{pmatrix} = \begin{pmatrix} \sqrt{1+\Sigma^2} \\ 0 \\ 0 \end{pmatrix} . \qquad (61)$$

Solutions for b_1, b_2, and r may be obtained in the following form:

$$b_1 = \frac{B_1 \sqrt{1+\Sigma^2}}{D} \qquad (62a)$$

$$b_2 = \frac{B_2 \sqrt{1+\Sigma^2}}{D} \qquad (62b)$$

$$r = \frac{B_3 \sqrt{1+\Sigma^2}}{D} \qquad (62c)$$

where

$$B_1 = v_2(\infty)\, u_3(0) - v_3(\infty) \qquad (63a)$$

$$B_2 = -[v_1(\infty)\, u_3(0) - v_3(\infty)] \qquad (63b)$$

$$B_3 = v_1(\infty) - v_2(\infty) \qquad (63c)$$

$$D = B_1 u_1(\Sigma) + B_2 u_2(\Sigma) + B_3 u_3(\Sigma) . \qquad (63d)$$

The absolute magnitudes of the solutions, Eqs. (62a,b,c,), pass through maxima and minima as Σ is varied, corresponding to resonances in the standing wave on the wire. The principal factor controlling the location and height of these maxima is the quantity $|D|$.

The complex factors B_n are constant for these relatively large values of Σ. In describing the total transverse motion of the wire according to Eq. (44), the term $b_1\, u_1(\sigma)$ can be represented by a vector which increases slowly in length with σ while rotating counterclockwise at a rate of

ν radians per unit of σ; the vector representation of $b_2\ u_2(\sigma)$ decreases slowly with σ while rotating clockwise at the same rate; and $r\ u_3(\sigma)$ decreases quite rapidly with σ, maintaining very nearly a constant angular position.

A numerical evaluation of the various quantities in Eqs. (63) shows that the third term in D is always considerably smaller than either of the other terms. Thus, the magnitude of the resultant D will be a minimum—*i.e.*, the response will be a maximum—when the first two terms are very nearly antiparallel. On the other hand, minimum responses (maximum $|D|$) will occur when the two dominant terms are nearly in phase.

The angular position of the third term is such that, in the minimum response condition, it is nearly parallel or antiparallel to the resultant of the first two terms. As a result, there are two classes of minima, which alternate as Σ varies, one lying on a higher envelope than the other. In the maximum response condition, however, the third term has practically no effect on the magnitude of D.

Of the greatest physical interest is the "worst" case (maximum response), which may be obtained by ignoring the third term in D entirely and treating the first two terms as antiparallel. Values of b_1, b_2, and r have been computed in this way for various values of Σ and ν, on the assumption that each input point is a node in the standing wave, regardless of the actual phase relationships at the point in question. The results have been shown in Tables II and III. In addition, Fig. 9(a), (b), (c), (d) shows the way in which the three waves combine at the origin.

TABLE II

TERMINATION	Σ	ν	b_1	b_2	r	$v(0)$
Fixed end	10	1	8.32 ∠-104.8°	12.86 ∠- 75.2°	22.5 ∠77.7°	0
		2	7.33 ∠-133.3°	8.97 ∠- 46.7°	46.8 ∠84.2°	0
		3	7.05 ∠-148.6°	7.87 ∠- 31.4°	65.5 ∠87.1°	0
		4	6.92 ∠-157.3°	7.40 ∠- 22.7°	83.8 ∠88.3°	0
		5	6.88 ∠-162.6°	7.19 ∠- 17.4°	100.5 ∠88.8°	0
Free end	10	1	6.77 ∠ 0°	6.77 ∠180°	0	6.49 ∠77.7°
		2	6.77 ∠ 0°	6.77 ∠180°	0	6.71 ∠84.2°
		3	6.77 ∠ 0°	6.77 ∠180°	0	5.11 ∠87.1°
		4	6.77 ∠ 0°	6.77 ∠180°	0	3.96 ∠88.3°
		5	6.77 ∠ 0°	6.77 ∠180°	0	3.11 ∠88.8°
Experimental System	10	1	7.78 ∠- 88.6°	10.98 ∠- 91.2°	20.5 ∠74.2°	2.51 ∠74.2°
		2	6.76 ∠- 88.7°	6.36 ∠- 91.3°	51.2 ∠78.8°	6.28 ∠78.8°
		3	6.22 ∠- 42.2°	4.60 ∠-137.8°	61.6 ∠91.3°	7.55 ∠91.3°
		4	6.63 ∠- 14.0°	6.21 ∠-166.0°	48.5 ∠95.0°	5.94 ∠95.0°
		5	6.70 ∠- 5.9°	6.47 ∠-174.1°	32.7 ∠94.2°	4.00 ∠94.2°

TABLE III

TERMINATION	Σ	ν	b_1	b_2	r	$v(0)$
Fixed end	5	3	$4.90 \angle -148.6°$	$5.47 \angle -31.4°$	$45.6 \angle 87.1°$	0
	10		$7.05 \angle -148.6°$	$7.87 \angle -31.4°$	$65.5 \angle 87.1°$	0
	15		$9.02 \angle -148.6°$	$10.18 \angle -31.4°$	$84.5 \angle 87.1°$	0
Free end	5	3	$4.60 \angle 0°$	$4.60 \angle 180°$	0	$3.47 \angle 87.1°$
	10		$6.77 \angle 0°$	$6.77 \angle 180°$	0	$5.11 \angle 87.1°$
	15		$8.73 \angle 0°$	$8.73 \angle 180°$	0	$6.59 \angle 87.1°$
Experimental system	5	3	$4.04 \angle -42.2°$	$2.99 \angle -137.8°$	$40.0 \angle 91.3°$	$4.90 \angle 91.3°$
	10		$6.22 \angle -42.2°$	$4.60 \angle -137.8°$	$61.6 \angle 91.3°$	$7.55 \angle 91.3°$
	15		$7.28 \angle -42.2°$	$5.39 \angle -137.8°$	$72.2 \angle 91.3°$	$8.84 \angle 91.3°$

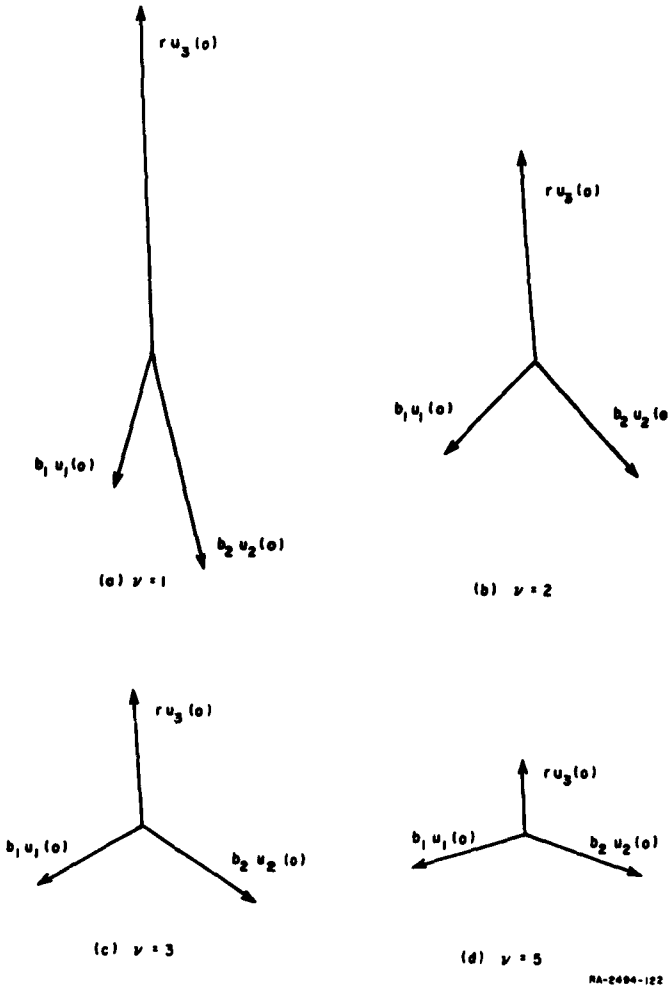

FIG. 9

SUPERPOSITION OF THREE WAVES AT FIXED LOWER END

D. TERMINATION WITH ZERO SPRING CONSTANT

If one postulates a cable termination consisting of a pre-stressed spring giving the proper value of equilibrium tension, but permitting longitudinal motion with a dynamic spring constant of zero, the boundary conditions are expressed by $\zeta_N = 0$, $r = 0$, $v(\Sigma) = 0$, and $w(\Sigma) = 1\underline{/0°}$. Although the tension variation r is zero, the longitudinal motion of the lower end of the cable, $v(0)$ [$= \zeta_p r$], is finite. For this case, Eqs. (78) may be written

$$\begin{pmatrix} u_1(\Sigma) & u_2(\Sigma) & 0 \\ v_1(\infty) & v_2(\infty) & -1 \\ 1 & 1 & 0 \end{pmatrix} \begin{pmatrix} b_1 \\ b_2 \\ v(0) \end{pmatrix} = \begin{pmatrix} \sqrt{1+\Sigma^2} \\ 0 \\ 0 \end{pmatrix} . \qquad (64)$$

The first and third components of Eq. (64) can be solved independently of the second, since Eq. (64) can also be written as follows:

$$\begin{pmatrix} u_1(\Sigma) & u_2(\Sigma) \\ 1 & 1 \end{pmatrix} \begin{pmatrix} b_1 \\ b_2 \end{pmatrix} = \begin{pmatrix} \sqrt{1+\Sigma^2} \\ 0 \end{pmatrix} \qquad (65a)$$

$$v(0) = b_1 v_1(\infty) + b_2 v_2(\infty) . \qquad (65b)$$

The solution of Eqs. (65a,b) gives

$$b_1 = \frac{\sqrt{1+\Sigma^2}}{u_1(\Sigma) - u_2(\Sigma)} \qquad (66a)$$

$$b_2 = -\frac{\sqrt{1+\Sigma^2}}{u_1(\Sigma) - u_2(\Sigma)} \qquad (66b)$$

$$v(0) = \sqrt{1+\Sigma^2}\left[\frac{v_1(\infty) - v_2(\infty)}{u_1(\Sigma) - u_2(\Sigma)}\right] . \qquad (66c)$$

It is seen that when the lower end of the wire is free to move longitudinally, there results a simpler type of transverse motion than if it is constrained, involving only u_1 and u_2. Maximum and minimum responses

in this case correspond exactly to nodes and antinodes in the standing wave pattern formed by the incident and reflected waves. Numerical results, again for the "worst" case, have been obtained and are shown for comparison in Tables II and III. The two waves are always equal in magnitude and 180° out of phase at the origin.

A clearer idea of what happens on the wire can be had by plotting the transverse amplitude as a function of position along the wire. The result, for $\Sigma = 10$, $\nu = 1$, and for both the fixed and free cases, is shown in Fig. 10. The amplitude, for the free-end case, oscillates between smooth upper and lower envelopes, given by

$$|w(\sigma)|_{max} = 6.77\sqrt{1+\sigma^2}\,(|u_1(\sigma)| + |u_2(\sigma)|) \qquad (67a)$$

$$|w(\sigma)|_{min} = 6.77\sqrt{1+\sigma^2}\,(|u_1(\sigma)| - |u_2(\sigma)|) \qquad (67b)$$

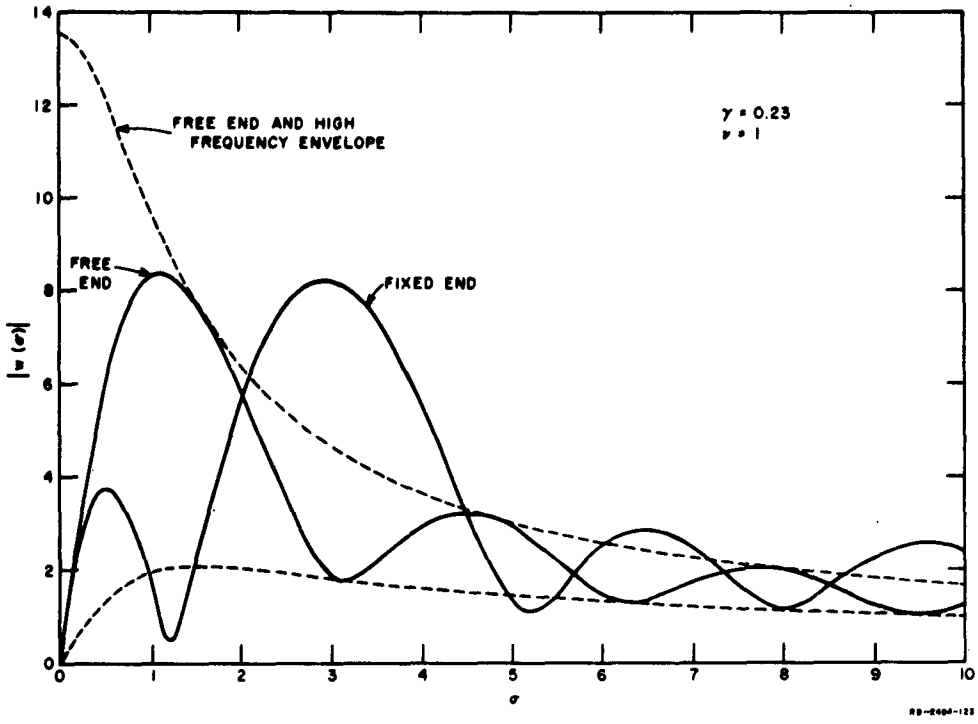

FIG. 10
VIBRATIONAL AMPLITUDE AS A FUNCTION OF POSITION ON THE WIRE FOR $\nu = 1$

At higher frequencies, the envelope remains the same, while the fluctuations of amplitude with position become increasingly rapid. The first maximum is always the highest, but can never exceed 13.54 times the input amplitude.

With the rigid termination, the three solutions combine in a complicated way in the lower part of the wire, yielding an amplitude pattern which does not necessarily stay within the same two envelopes. The exact nature of this pattern is dependent upon frequency, and it is possible for the second maximum to be as high as about 20 times the input amplitude at some frequencies. At points farther up along the cable, the standing wave has much the same appearance as in the free-end case, except for a phase shift of the maxima and minima relative to their former positions, and a somewhat greater fluctuation in amplitude due to the presence of a larger proportion of u_2 than before. The effect of u_3 decreases markedly at higher frequencies, and the whole pattern approaches that which is obtained for the free case.

It should be noted that, although the transverse amplitude patterns in the two extreme cases are the same at high frequencies, the longitudinal motion and tension fluctuation are quite different. In the free case the tension, of course, remains constant, while there is considerable longitudinal motion of the lower end of the cable, decreasing at the higher frequencies; in the fixed case there is no motion of the lower end, but the tension variation becomes progressively more severe with increasing frequency.

E. OTHER TERMINATIONS

It is possible to consider many other theoretical terminations, including viscous types capable of absorbing energy. Since two constants, ζ_N and ζ_P, are needed to describe the termination completely, it is possible, at a given frequency and for a particular set of flight parameters, to satisfy two independent conditions. It is not difficult to show that

$$\zeta_{NP} = G \left[\frac{(\nu_{NP}^2 - \alpha_{NP}^2) + i\alpha_{NP}\nu}{1 + \frac{\alpha_{NP}^2}{\nu^2}} \right]^{-1} \quad . \tag{68}$$

In Eq. (68), G represents the acceleration of gravity in consistent dimensionless units, and α_{NP} is a dimensionless coefficient of viscous

friction in the N or P direction. These quantities are defined mathematically as follows:

$$G = \frac{gC}{U^2} \quad , \tag{69}$$

$$\alpha_{NP} = \frac{\mu_{NP} C}{mU} \quad , \tag{70}$$

where μ_{NP} is the coefficient of viscous friction in conventional units—e.g., lb-sec/ft. The frequency ν_{NP} is the (dimensionless) natural frequency of the weight and its suspension, and m is the mass of the weight.

For the actual experimental system using a pre-stressed spring, the flight-test conditions and the constants of the linkage are such that

$$\left.\begin{aligned} G &= 2.07 \times 10^{-3} \quad , \quad \nu_N \approx \infty \\ \nu_P &\approx 0.13 \quad , \quad \alpha_P \approx 0 \quad . \end{aligned}\right\}$$

These values lead to the following:

$$\zeta_N \approx 0 \quad , \quad \zeta_P \approx 0.123 \angle 0^\circ \quad .$$

Numerical results in the computation of $w(\sigma)$ are shown for comparison in Tables II and III. It is seen that this termination is very much like the fixed case at low frequencies, and very much like the free case at high frequencies. It is possible however, at certain frequencies, to have either longitudinal amplitudes greater than in the free case or tension fluctuations greater than in the fixed case.

The longitudinal amplitudes have been shown as functions of frequency in Fig. 11 for a wire of $\Sigma = 10$ and fixed input amplitude of 10^{-3} in dimensionless units, corresponding to 0.063 in. in this case. For some purposes it is of greater interest to know the longitudinal response for a fixed acceleration. This has been shown in Fig. 12 for a dimensionless acceleration amplitude of 10^{-2}, corresponding to 4.82 g. The amplitudes of the tension fluctuation, in percent, have been shown for the same conditions in Figs. 13 and 14. It is worthy of note that, for amplitudes of such size that the cable never goes slack, the motion of the lower end of

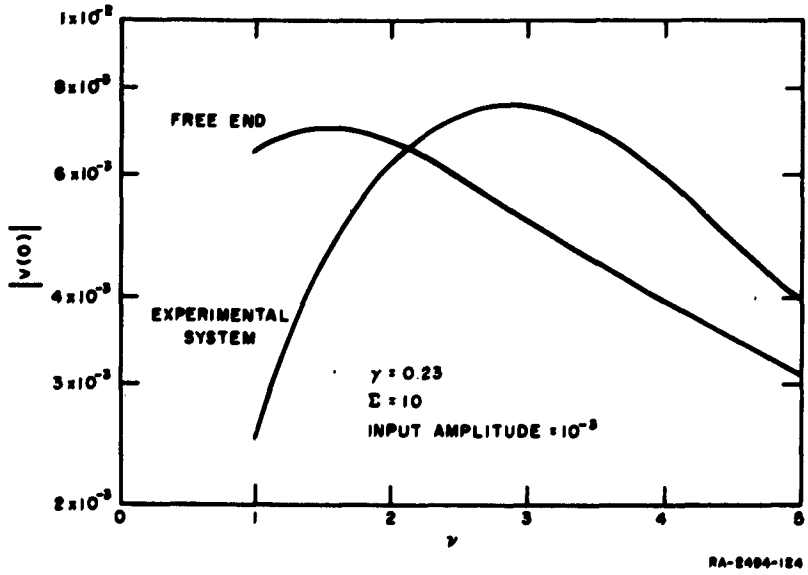

FIG. 11

LONGITUDINAL AMPLITUDE AT LOWER END OF CABLE WITH FIXED INPUT AMPLITUDE

the cable due to the second-order effect described in Sec. II-G can be neglected in comparison with the first-order effect.

It would be at least theoretically possible in this same system under a particular set of flight conditions, to eliminate both the return wave u_2 and the "tension wave" u_3. First, the tension wave can be eliminated by making $\zeta_p = \infty$ as already described. There are, however, considerable practical difficulties attendant upon designing a springing arrangement to give the correct static tension, to center properly, and still to be much "softer" dynamically than that which is used in the experimental system. Second, u_2 may be eliminated by making

$$\zeta_N = (\gamma + i\nu)^{-1} \quad , \tag{71}$$

leaving a pure traveling wave on the wire. Reference to Eq. (68) and consideration of the magnitudes involved show that this may be achieved if

$$\alpha_N \approx G \tag{72a}$$

$$\nu_N \approx \sqrt{G\,(\gamma + G)} \quad . \tag{72b}$$

The result is independent of frequency, but the values of spring and damping constants required in the suspension in order that Eq. (72a,b) be satisfied depend upon airspeed and altitude. Such an arrangement is therefore of rather doubtful utility. It should be remembered also that the method of suspension described above fails entirely to eliminate the longitudinal motion.

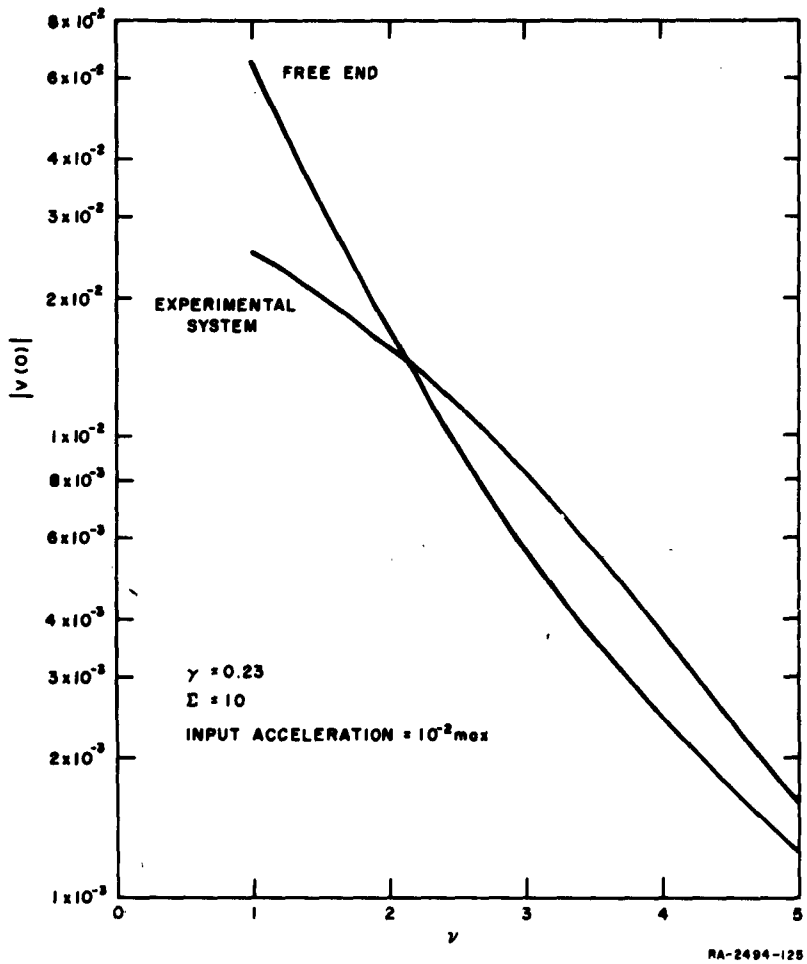

FIG. 12

LONGITUDINAL AMPLITUDE AT LOWER END OF CABLE WITH FIXED INPUT ACCELERATION

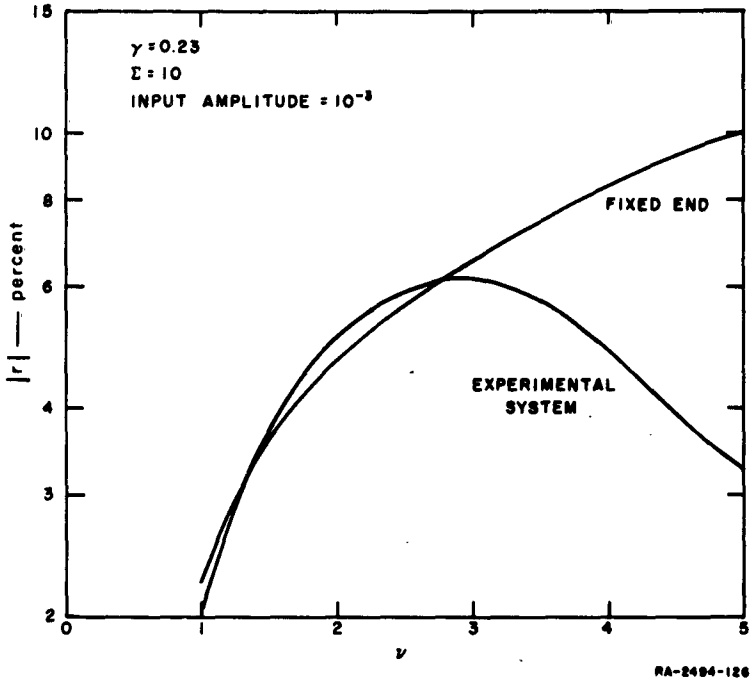

FIG. 13

TENSION FLUCTUATION IN CABLE WITH FIXED INPUT AMPLITUDE

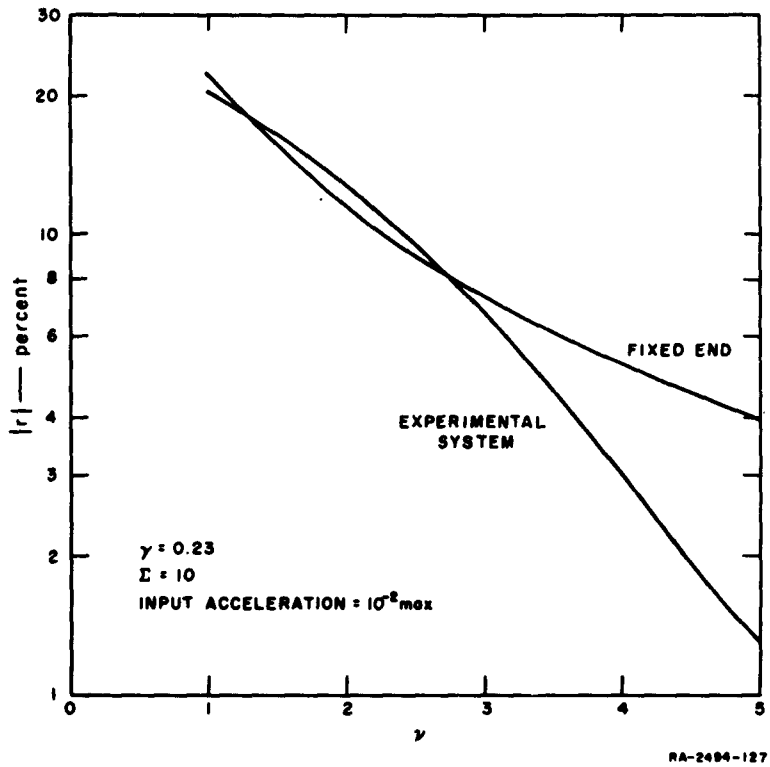

FIG. 14

TENSION FLUCTUATION IN CABLE WITH FIXED INPUT ACCELERATION

V SUMMARY AND CONCLUSIONS

In summary it can be said that the aerodynamic characteristics of trailing wires at both subsonic and supersonic speeds are well understood. In particular, the factors leading to cable failure are known and have been subjected to mathematical analysis. Investigation of various means for control of the undesirable phenomena indicates a strong possibility that trailing-wire antennas may be practical even for supersonic aircraft.

The static shape of a trailing cable can be described very closely for all speed-altitude combinations by a single dimensionless expression. The mechanical waves which can exist on the wire have also been described in dimensionless form. The theory developed in this report expresses the motion in terms of an amplified wave traveling downwind, a damped wave traveling upwind, and a standing wave resulting from wire curvature and existing primarily in regions where the curvature is large. On this same highly curved portion of the cable there is a tendency for the transverse oscillations to give rise to longitudinal oscillations. If the longitudinal motion is restrained in any way, first-order fluctuations in tension result.

The lower end of a trailing antenna can be stabilized through the use of a heavy, aerodynamically stable end-weight of low drag. Under these conditions, the most important vibratory inputs are those at or near the upper end of the wire, and the crucial factor determining system instability is the aerodynamic amplification experienced by the downwind wave. The high value of cable tension limits the amplification to a relatively low figure, but cannot eliminate it entirely at supersonic speeds without exceeding the breaking stress of the cable.

The theory described in this report was applied to the design of an experimental system which has been successfully flown at speeds as high as Mach 1.24. The theoretical amplification in the worst flight-test condition was about 8, and the tension fluctuations were calculated to be of the order of 20 percent for liberally assumed vibratory inputs. The tests showed clearly that this degree of aerodynamic amplification is tolerable, as the observed tension fluctuations attributable to the phenomena discussed in

this report were relatively slight. Tension variations resulting from other causes were observed, but none was of sufficient magnitude to bring about failure of the antenna in flight. A practical antenna for use on Mach 2 to Mach 3 aircraft would have maximum amplification of the same order of magnitude as the experimental system. Although the indications are favorable, the question of the stability of such a higher-speed installation can be finally settled only through appropriate flight testing.

APPENDIX A

EQUATIONS OF THE CABLE SHAPE IN TERMS OF THE DIMENSIONLESS VARIABLES ξ, η, σ, AND ϕ FOR ZERO-DRAG END-WEIGHT

APPENDIX A

EQUATIONS OF THE CABLE SHAPE IN TERMS OF THE DIMENSIONLESS VARIABLES ξ, η, σ, AND ϕ FOR ZERO-DRAG END-WEIGHT

VARIABLE	IN TERMS OF ξ	IN TERMS OF η	IN TERMS OF σ	IN TERMS OF ϕ
ξ	---	$\cosh \eta - 1$	$\sqrt{1 + \sigma^2} - 1$	$\csc \phi - 1$
η	$\cosh^{-1} (1 + \xi)$	---	$\sinh^{-1} \sigma$	$\ln \cot (\phi/2)$
σ	$\sqrt{\xi(2 + \xi)}$	$\sinh \eta$	---	$\cot \phi$
ϕ	$\csc^{-1} (1 + \xi)$	$\cot^{-1} (\sinh \eta)$	$\cot^{-1} \sigma$	---

APPENDIX B

WAVE MOTION IN THE CABLE AT ZERO ANGLE OF ATTACK

APPENDIX B

WAVE MOTION IN THE CABLE AT ZERO ANGLE OF ATTACK

1. THE NON-LINEAR EQUATION OF MOTION

The theory given in Sec. III for wave motion on a wire immersed in an airstream is not applicable at very small angles between wind and wire. The purpose of this Appendix is to develop an approximate theory which is valid when the wind direction is exactly parallel to the cable. Before proceeding, however, it is convenient to describe a mathematical development which will be needed.

Consider the function

$$y(x) = |\sin x| \sin x \qquad \text{(B-1)}$$

shown in Fig. B-1. This function can be expanded in a Fourier series as follows:

$$y(x) = \sum_{k=1}^{\infty} a_k \sin kx \quad . \qquad \text{(B-2)}$$

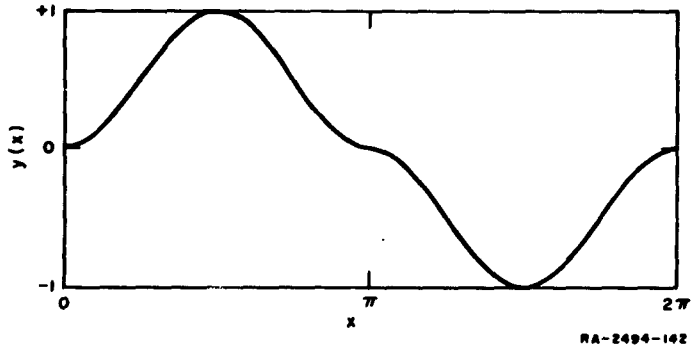

FIG. B-1
THE FUNCTION $y(x) = |\sin x| \sin x$

Only odd harmonics are present, and their coefficients are given by

$$a_k = -\frac{8}{k\,(k^2-4)\,\pi} \quad . \tag{B-3}$$

Numerically,

$$a_{1,3,5\ldots} = \frac{8}{3\pi} \;,\; -\frac{8}{15\pi} \;,\; -\frac{8}{105\pi} \;\ldots\ldots \tag{B-4}$$

The coefficients of the higher harmonics decrease approximately as the inverse cube of k.

Now, for slope angles ϕ in the neighborhood of $\phi_0 = 0$, the second term of Eq. (22) cannot be neglected in comparison with the first, and the approximation of Eq. (23) does not hold. The angle ϕ, however, may be approximated as follows:

$$\phi = \sin\phi = \tan\phi = \frac{\partial n}{\partial s} \quad . \tag{B-5}$$

The aerodynamic force on an element of cable is proportional in magnitude to V_n^2 and has the same algebraic sign as V_n. It may be written in the following form:

$$dF = f(s,t)\; T\; ds \tag{B-6}$$

where

$$f(s,t) = \frac{1}{C}\left|\frac{V_n}{V_0}\right|\frac{V_n}{V_0} \quad . \tag{B-7}$$

Substitution into Eq. (24) gives for the equation of transverse motion

$$\frac{\partial^2 n}{\partial s^2} - \frac{1}{U^2}\,\frac{\partial^2 n}{\partial t^2} + f(s,t) = 0 \quad . \tag{B-8}$$

To obtain an approximate solution of (B-8) in a particular case where damping is known to be small, an undamped solution is used to evaluate V_n, and thence the small term $f(s,t)$. The damped solution is then computed from the resulting equation.

2. TRAVELING WAVES

Suppose that the solution desired is that of a traveling wave in the downwind direction, excited sinusoidally at the origin. The dependence on time must be harmonic, and a solution of the form

$$n = u(s) \sin \omega \left(t + \frac{s}{U} \right) \tag{B-9}$$

is assumed, where $u(s)$ is real and slowly-varying. Then

$$\frac{V_n}{V_0} = \frac{\partial n}{\partial s} - \frac{1}{V_0} \frac{\partial n}{\partial t} \tag{B-10}$$

or, if the term in the derivative of u is neglected,

$$\frac{V_n}{V_0} = \frac{\omega u}{U} (1 - \gamma) \sin \left[\omega \left(t + \frac{s}{U} \right) + \frac{\pi}{2} \right] . \tag{B-11}$$

Also,

$$f(s,t) = \frac{1}{C} \left(\frac{\omega u}{U} \right)^2 (1 - \gamma)^2 \, y \left[\omega \left(t + \frac{s}{U} \right) + \frac{\pi}{2} \right] \tag{B-12}$$

which, by Eqs. (B-2) and (B-3), is seen to consist of a Fourier series whose fundamental leads the displacement by 90 degrees.

With this linearization, Eq. (B-8) can now be treated more conveniently with complex numbers. Since the complete solution must also be periodic in time, although higher harmonics may be present, it will be taken to be of the form

$$n = \sum_{\substack{k=1 \\ odd}}^{\infty} u_k(s) \, \epsilon^{ik\omega(t+s/U)} . \tag{B-13}$$

The boundary condition at the origin is

$$n(0,t) = n_0 \, \epsilon^{i\omega t} \tag{B-14}$$

and therefore

$$u_k(0) = n_0 \qquad (k = 1) \tag{B-15a}$$

$$u_k(0) = 0 \qquad (k \neq 1) \quad . \tag{B-15b}$$

Equation (B-8) can now be written as

$$\frac{\partial^2 n}{\partial s^2} - \frac{1}{U^2}\frac{\partial^2 n}{\partial t^2} = -\left(\frac{\omega u_1}{U}\right)^2 \frac{(1-\gamma)^2}{C} \sum_{\substack{k=1 \\ odd}}^{\infty} a_k \, e^{ik\omega(t+s/U)} \, e^{ik\pi/2} \tag{B-16}$$

or

$$\frac{\partial^2 n}{\partial s^2} - \frac{1}{U^2}\frac{\partial^2 n}{\partial t^2} = i\left(\frac{\omega u_1}{U}\right)^2 \frac{(1-\gamma)^2}{C} \sum_{\substack{k=1 \\ odd}}^{\infty} (-1)^{\frac{1}{2}(k+1)} \, a_k \, e^{ik\omega(t+s/U)} \tag{B-17}$$

where the a_k are given by Eq. (B-3). When (B-13) is substituted in (B-17), the resulting equation must be satisfied component by component, and we have

$$\frac{d^2 u_k}{ds^2} + i\,2k\,\frac{\omega}{U}\,\frac{du_k}{ds} = i\,\frac{1}{C}\left(\frac{\omega u_1}{U}\right)^2 (1-\gamma)^2\,(-1)^{\frac{1}{2}(k+1)}\,a_k \quad . \tag{B-18}$$

The amplitudes u_k will be assumed to be sufficiently slowly-varying that

$$\frac{d^2 u_k}{ds^2} \ll 2k\,\frac{\omega}{U}\,\frac{du_k}{ds} \quad . \tag{B-19}$$

Then Eq. (B-18) can be rewritten to give the following set of equations:

$$\frac{du_k}{ds} = (-1)^{\frac{1}{2}(k+1)}\,\frac{\omega(1-\gamma)^2}{2kCU}\,a_k\,u_1^2 \quad . \tag{B-20}$$

In particular, for $k = 1$, Eq. (B-20) becomes

$$\frac{du_1}{ds} = -\frac{4\omega(1-\gamma)^2}{3\pi CU} u_1^2 \quad , \tag{B-21}$$

which can be integrated directly to give

$$\frac{u_1(s)}{n_0} = \left[1 + \frac{4\omega(1-\gamma)^2 n_0}{3\pi CU} s\right]^{-1} \quad . \tag{B-22}$$

If the foregoing is substituted in Eq. (B-20), the amplitudes for $k \neq 1$ can be found:

$$\frac{u_k(s)}{n_0} = (-1)^{\frac{1}{2}(k-1)} \frac{3}{k^2(k^2-4)} \left\{1 - \left[1 + \frac{4\omega(1-\gamma)^2 n_0}{3\pi CU} s\right]^{-1}\right\} \quad . \tag{B-23}$$

In dimensionless units the complete solution can be written:

$$\frac{N(\sigma,\tau)}{N_0} = \left[1 + \frac{4}{3\pi}(1-\gamma)^2 \nu N_0 \sigma\right]^{-1} \epsilon^{i\nu(\tau+\sigma)} + \left\{1 - \left[1 + \frac{4}{3\pi}(1-\gamma)^2 \nu N_0 \sigma\right]^{-1}\right\} \sum_{\substack{k=3 \\ \text{odd}}}^{\infty} (-1)^{\frac{1}{2}(k-1)} \frac{3}{k^2(k^2-4)} \epsilon^{ik\nu(\tau+\sigma)} \quad . \tag{B-24}$$

Equation (B-24) shows that the fundamental component of the wave is amplified, although not exponentially, with distance along the wire, while small amounts of higher harmonics are created. A similar investigation of an upwind wave gives, under the same conditions,

$$\frac{N(\sigma,\tau)}{N_0} = \left[1 + \frac{4}{3\pi}(1+\gamma)^2 \nu N_0 \sigma\right]^{-1} \epsilon^{i\nu(\tau-\sigma)} + \left\{1 - \left[1 + \frac{4}{3\pi}(1+\gamma)^2 \nu N_0 \sigma\right]^{-1}\right\} \sum_{\substack{k=3 \\ \text{odd}}}^{\infty} (-1)^{\frac{1}{2}(k-1)} \frac{3}{k^2(k^2-4)} \epsilon^{ik\nu(\tau-\sigma)} \tag{B-25}$$

from which it can be seen that this wave is attenuated with distance.

3. STANDING WAVE

Because of the nonlinearity of Eq. (B-8), it is not possible to superpose the traveling-wave solutions given in Eqs. (B-24) and (B-25) to obtain a standing-wave solution. Let the case where complete reflection at the origin occurs be considered. The initial solution will be taken to be

$$n = n_a \sin \frac{\omega s}{U} \sin \omega t \qquad \text{(B-26)}$$

where n_a is real, positive and constant.

Using Eq. (B-10), one finds

$$\frac{V_n}{V_0} = \frac{n_a \omega}{U} \left[\cos^2 \frac{\omega s}{U} + \gamma^2 \sin^2 \frac{\omega s}{U} \right]^{1/2} \sin (\omega t - \psi) \qquad \text{(B-27)}$$

where

$$\psi = \tan^{-1} \left[\gamma \tan \frac{\omega s}{U} \right] . \qquad \text{(B-28)}$$

In this case the fundamental component of $f(s,t)$ lags the displacement by the angle ψ, and we can write

$$f(s,t) = \frac{1}{C} \left(\frac{n_a \omega}{U} \right)^2 \left[\cos^2 \frac{\omega s}{U} + \gamma^2 \sin^2 \frac{\omega s}{U} \right] y(\omega t - \psi) . \qquad \text{(B-29)}$$

The complete solution will be taken to be, in complex notation,

$$n = \sum_{\substack{k=1 \\ odd}}^{\infty} \left[b_k \sin \left(k \frac{\omega s}{U} \right) + u_k(s) \cos \left(k \frac{\omega s}{U} \right) \right] \epsilon^{ik\omega t} . \qquad \text{B-30)}$$

If the system is excited sinusoidally at the point $s = S$—that is, if

$$n(S,t) = n_0 \epsilon^{i\omega t} , \qquad \text{(B-31)}$$

the boundary conditions become

$$u_k(0) = 0 \qquad \text{(B-32a)}$$

$$b_k = n_a \qquad (k = 1) \qquad \text{(B-32b)}$$

$$b_k = -u_k(S) \cot\left(k\frac{\omega S}{U}\right) \qquad (k \neq 1) \qquad \text{(B-32c)}$$

$$n_a \sin\frac{\omega S}{U} + u_1(S)\cos\frac{\omega S}{U} = n_0 \qquad \text{(B-32d)}$$

With the use of Eq. (B-29), Eq. (B-8) can be written

$$\frac{\partial^2 n}{\partial s^2} - \frac{1}{U^2}\frac{\partial^2 n}{\partial t^2} = -\frac{1}{C}\left(\frac{n_a\omega}{U}\right)^2\left[\cos^2\frac{\omega s}{U} + \gamma^2\sin^2\frac{\omega s}{U}\right]\sum_{\substack{k=1\\ \text{odd}}}^{\infty} a_k\, \epsilon^{ik\omega t}\,\epsilon^{-ik\psi} \quad . \qquad \text{(B-33)}$$

As in the case of the traveling wave, substitution of Eq. (B-30) into (B-33) leads to a set of equations for the individual components:

$$\frac{d^2u_k}{ds^2}\cos\left(k\frac{\omega s}{U}\right) - 2k\,\frac{\omega}{U}\,\frac{du_k}{ds}\sin\left(k\frac{\omega s}{U}\right) = -\frac{a_k}{C}\left(\frac{n_a\omega}{U}\right)^2\left[\cos^2\frac{\omega s}{U} + \gamma^2\sin^2\frac{\omega s}{U}\right]\epsilon^{-ik\psi} \quad . \qquad \text{(B-34)}$$

Let the function $v_k(s)$ be defined as follows:

$$v_k(s) = v_{kr}(s) + i\,v_{ki}(s) = \frac{du_k}{ds}\cos^2\left(k\frac{\omega s}{U}\right) . \qquad \text{(B-35)}$$

Then Eq. (B-34) can be written

$$\frac{dv_k}{ds} = -\frac{a_k}{C}\left(\frac{n_a\omega}{U}\right)^2\left[\cos^2\frac{\omega s}{U} + \gamma^2\sin^2\frac{\omega s}{U}\right]\left[\cos k\psi - i\sin k\psi\right]\cos\left(k\frac{\omega s}{U}\right) . \qquad \text{(B-36)}$$

Since $v_k(\pi U/2\omega)$ must be zero, the real and imaginary parts of v_k are

$$v_{kr}(s) = -\frac{a_k}{C}\left(\frac{n_a\omega}{U}\right)^2\int_{\pi U/2\omega}^{s}\left[\cos^2\frac{\omega s}{U} + \gamma^2\sin^2\frac{\omega s}{U}\right]\cos\left(k\frac{\omega s}{U}\right)\cos k\psi\, ds \qquad \text{(B-37a)}$$

$$v_{k1}(s) = \frac{a_k}{C}\left(\frac{n_s\omega}{U}\right)^2 \int_{\pi U/2\omega}^{s} \left[\cos^2\frac{\omega s}{U} + \gamma^2 \sin^2\frac{\omega s}{U}\right] \cos\left(k\frac{\omega s}{U}\right) \sin k\psi \, ds \quad . \tag{B-37b}$$

Now, from Eq. (B-32a) $u_k(0)$ must be zero, and therefore Eq. (B-35) can be integrated to give

$$u_k(S) = \int_0^S v_k(s) \sec^2\left(k\frac{\omega s}{U}\right) ds \quad . \tag{B-38}$$

The evaluation of $u_k(S)$ in the general case requires two successive numerical integrations for each value of γ which is of interest. However, there is one important special case for which the problem is greatly simplified. Since the integrands of Eqs. (B-37a) and (B-37b) have symmetry and antisymmetry, respectively, about the point $s = \pi U/2\omega$, the corresponding integrals have the reverse properties. Consequently, when the cable length S is equal to an integral number of half-wavelengths the real part of $u_k(S)$ vanishes in the integration of Eq. (B-38). The imaginary part of $v_k(s)$, unlike the real part, can be found analytically, and u_k for any value of γ is computed by means of a single numerical integration.

The amplitude of harmonics other than the first cannot be found in this special case by the method under discussion, because of the appearance of cot π in Eq. (B-32c). (In principle, the inclusion of higher order terms in Eq. (B-33) would have yielded this information.) Results for the fundamental, however, are obtainable and will be given here. Integration of Eq. (B-37b) for $k = 1$ gives

$$v_{1i} = \frac{8\omega n_s^2}{9\pi CU(1-\gamma^2)}\left[\gamma^3 - \left(\cos^2\frac{\omega s}{U} + \gamma^2 \sin^2\frac{\omega s}{U}\right)^{3/2}\right] \tag{B-39}$$

and, taking into account the fact that the positive 3/2-power must always be used, Eq. (B-38) reduces to

$$u_1(S) = -ip\frac{n_s^2}{C} q(\gamma) \quad . \tag{B-40}$$

The index p gives the number of half-wave loops, and $q(\gamma)$ is defined by

$$q(\gamma) = \frac{16}{9\pi(1-\gamma^2)} \int_0^{\pi/2} [(\cos^2\theta + \gamma^2 \sin^2\theta)^{3/2} - \gamma^3] \sec^2\theta \, d\theta \quad . \tag{B-41}$$

Numerical values of $q(\gamma)$ are shown graphically in Fig. B-2.

The information of greatest interest from the point of view of design is the relationship between the excitation n_0 and the first-harmonic response n_a. In the case of half-wave resonance, Eq. (B-32d) shows that $n_0 = u_1(S)$, and we can write

$$n_a = \sqrt{p\, q(\gamma)} \cdot \sqrt{C\,|n_0|} \quad . \tag{B-42}$$

The standing wave amplitude is seen to be proportional to the square root of the input amplitude.

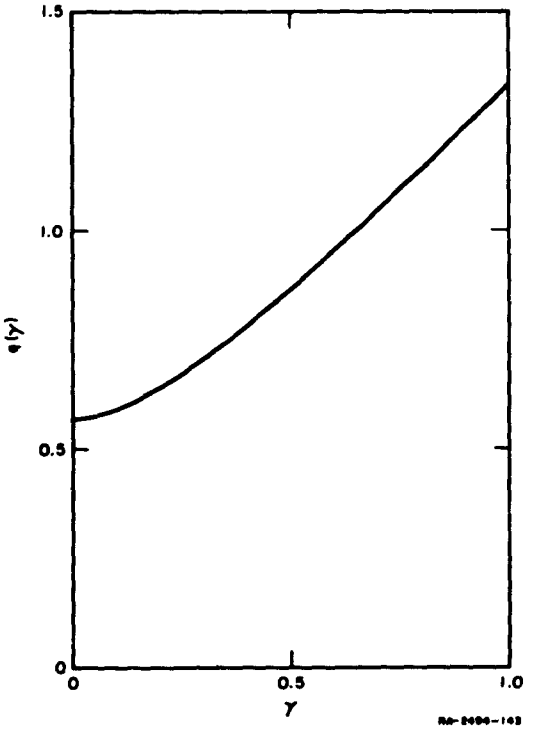

FIG. B-2
THE FUNCTION q(γ)

APPENDIX C

VARIATION OF WIRE LENGTH DUE TO STANDING WAVE

APPENDIX C

VARIATION OF WIRE LENGTH DUE TO STANDING WAVE

If the first-order wave on the wire is known, it is possible to obtain an approximate expression for the variation of over-all wire length with time. Let ds_0 be the length of an element of the distorted wire, n its displacement normal to its equilibrium direction, and ds its projection on that same direction. Then

$$ds = \left[1 + \left(\frac{\partial n}{\partial s_0}\right)^2\right]^{-\frac{1}{2}} ds_0 \quad . \tag{C-1}$$

Note that n here represents the actual instantaneous value of the displacement, not its complex value, which is meaningful only in the first-order theory. For moderate amplitudes, Eq. (C-1) can be expanded as follows:

$$ds = \left[1 - \frac{1}{2}\left(\frac{\partial n}{\partial s_0}\right)^2\right] ds_0 \quad . \tag{C-2}$$

For a single cycle of a sinusoid of amplitude a and wavelength λ on a straight wire, it is easy to show by integration of the above that

$$\frac{S}{S_0} = 1 - \left(\frac{\pi a}{\lambda}\right)^2 \quad . \tag{C-3}$$

Now the instantaneous transverse displacement along the curved wire is given by the real part of Eq. (17). If the time origin is chosen to make a_1 real, and total reflection is assumed, the result is

$$Re[n] = a_1\left[A_1^{-1}\cos\omega\left(\frac{C\sigma_0}{U} + t\right) - A_2^{-1}\cos\omega\left(\frac{C\sigma_0}{U} - t\right)\right] \quad . \tag{C-4}$$

This equation can be rewritten as follows:

$$Re[n] = a(\sigma_0, t) \cos\left(\omega \frac{C\sigma_0}{U} + \psi\right) , \qquad \text{(C-5)}$$

where

$$a(\sigma_0, t) = a_1 \left[A_1^{-2} + A_2^{-2} - 2A_1^{-1} A_2^{-1} \cos 2\omega t\right]^{1/2} \qquad \text{(C-6)}$$

and

$$\psi(\sigma_0, t) = \tan^{-1}\left[\frac{A_2 + A_1}{A_2 - A_1} \tan \omega t\right] . \qquad \text{(C-7)}$$

At any given instant of time, Eq. (C-5) represents a sinusoid with amplitude and phase varying along the cable. For waves of sufficiently short wavelength, this variation will be negligible over one wavelength, and the contraction of the wire can be considered as the sum of a number of small contractions in which the local length decreases by the factor given in Eq. (C-3). Then it is possible to write

$$\Sigma = \int_0^{\Sigma_0} \left[1 - \left(\frac{\pi a}{\lambda}\right)^2\right] d\sigma_0 , \qquad \text{(C-8)}$$

or

$$\Sigma = \Sigma_0 - \left(\frac{\pi a_1}{\lambda}\right)^2 \int_0^{\Sigma_0} \left[A_1^{-2} + A_2^{-2} - 2A_1^{-1} A_2^{-1} \cos 2\omega t\right] d\sigma_0 . \qquad \text{(C-9)}$$

The first two terms in the integral, which can be evaluated numerically in a particular case if desired, are not of any physical interest, as they represent only a static change in the equilibrium length. It is the third, or time-dependent, term which gives the amplitude of the fluctuation. This amplitude is easily seen to be

$$\Sigma' = 2\left(\frac{\pi a_1}{\lambda}\right)^2 \int_0^{\Sigma_0} \frac{d\sigma_0}{A_1 A_2} = 2\left(\frac{\pi a_1}{\lambda}\right)^2 \int_0^{\Sigma_0} \frac{d\sigma_0}{1 + \sigma_0^2} \quad , \qquad \text{(C-10)}$$

or

$$\Sigma' = 2\left(\frac{\pi a_1}{\lambda}\right)^2 \tan^{-1} \Sigma_0 \quad . \qquad \text{(C-11)}$$

APPENDIX D

VALIDITY OF EQUATION (41) AND ANALYTIC EXPRESSIONS FOR THE HOMOGENEOUS SOLUTIONS

APPENDIX D

VALIDITY OF EQUATION (41) AND ANALYTIC EXPRESSIONS FOR THE HOMOGENEOUS SOLUTIONS

The purpose of this Appendix is to determine the range of conditions under which Eq. (41) is a good approximation, and then to find an analytic representation of the integral.

Differentiation of Eq. (41) gives

$$u'' = -\nu^2 f\, u\left[1 - i\left(\frac{f'}{2\nu f^{3/2}}\right)\right] . \tag{D-1}$$

The condition that Eq. (41) be a good solution is evidently that

$$\left|\frac{f'}{2\nu f^{3/2}}\right| \ll 1 \tag{D-2}$$

or say

$$\left|\frac{f'}{2\nu f^{3/2}}\right| < 10^{-1} . \tag{D-3}$$

The quantity on the left-hand side of Eq. (D-3) always has a maximum for some value of σ. If this maximum is less than 10^{-1}, then the approximate solution is valid for all values of σ. Based on this fact, it is possible to find for any value of γ a critical value of ν below which the approximation of Eq. (41) fails. The resulting curve is shown in Fig. (D-1), and will be referred to as Criterion A.

The evaluation of the integral appearing in Eq. (41) is greatly simplified if $[1 - 2i\,(\gamma/\nu)(1 + \sigma^2)^{-1/2}]^{1/2}$ can be expanded in powers of $2(\gamma/\nu)(1 + \sigma^2)^{-1/2}$. The first few terms in the expansion are

$$\sqrt{f(\sigma)} = 1 - i(\gamma/\nu)(1 + \sigma^2)^{-1/2} + \frac{1}{2}(\gamma/\nu)^2\,(1 + \sigma^2)^{-1} + \frac{1}{2}\,i(\gamma/\nu)^3\,(1 + \sigma^2)^{-3/2} - \frac{5}{8}(\gamma/\nu)^4\,(1 + \sigma^2)^{-2} + \ldots . \tag{D-4}$$

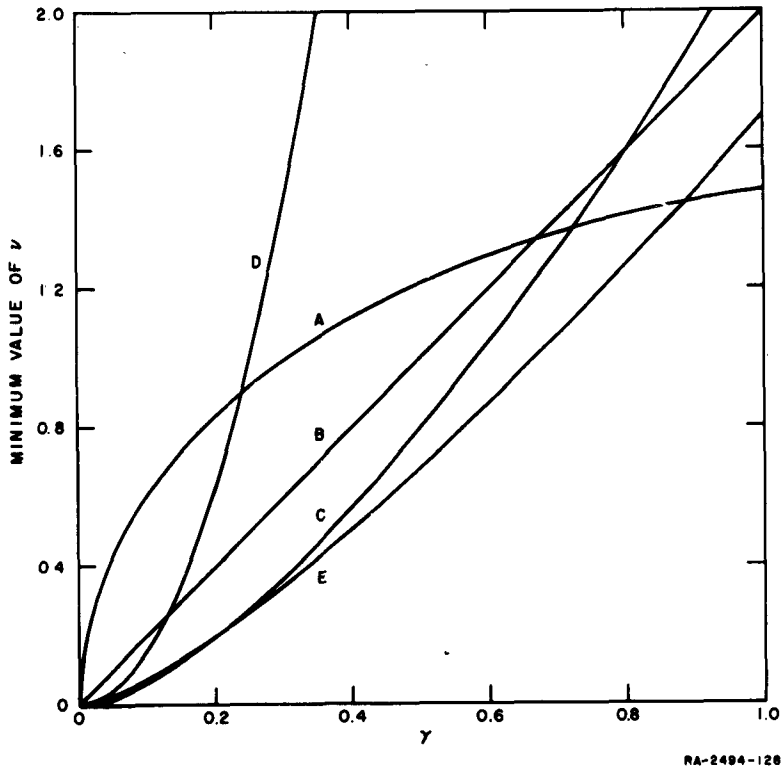

FIG. D-1

CRITERIA RELATING TO THE APPROXIMATE SOLUTION OF EQUATION (39)

Careful testing of the real and imaginary parts of this series yields the result that for convergence at the worst point ($\sigma = 0$) one must have

$$\nu > 2\gamma \qquad \text{(Criterion B)} \quad . \tag{D-5}$$

This criterion may be seen from Fig. (D-1) to be less restrictive than Criterion A for values of γ less than 0.67, and more restrictive for $\gamma > 0.67$.

The imaginary part of (D-4), when integrated, leads to multiplicative factors in the amplitude of the wave, while the real part leads to additive terms in the phase. To ascertain how many terms of Eq. D-4 are needed, the integral must be evaluated term by term. The result is

$$i\nu \int_0^\sigma \sqrt{f(\sigma')}\, d\sigma' = i\nu \left[\sigma + \frac{1}{2}\left(\frac{\gamma}{\nu}\right)^2 \tan^{-1}\sigma - \frac{5}{16}\left(\frac{\gamma}{\nu}\right)^4 \left(\frac{\sigma}{1+\sigma^2} + \tan^{-1}\sigma\right) + \ldots\right]$$

$$+ \gamma \left[\ln\left(\sigma + \sqrt{1+\sigma^2}\right) - \frac{1}{2}\left(\frac{\gamma}{\nu}\right)^2 \frac{\sigma}{\sqrt{1+\sigma^2}} + \ldots\right] \quad . \tag{D-6}$$

The two independent homogeneous solutions of Eq. (39) thus become

$$u_1(\sigma) = \left(\sigma + \sqrt{1+\sigma^2}\right)^{\gamma} \epsilon^{i\nu\sigma} \left[g(\sigma)\, \epsilon^{ih(\sigma)}\right] \tag{D-7a}$$

$$u_2(\sigma) = \left(\sigma + \sqrt{1+\sigma^2}\right)^{-\gamma} \epsilon^{-i\nu\sigma} \left[\epsilon^{-ih(\sigma)}/g(\sigma)\right] \tag{D-7b}$$

where

$$g(\sigma) = \exp\left(-\frac{\gamma^3}{2\nu^2} \frac{\sigma}{\sqrt{1+\sigma^2}} + \ldots\right) \tag{D-8a}$$

$$h(\sigma) = \frac{\gamma^2}{2\nu} \tan^{-1}\sigma - \frac{5}{16}\frac{\gamma^4}{\nu^3} \left(\frac{\sigma}{1+\sigma^2} + \tan^{-1}\sigma\right) + \ldots \quad . \tag{D-8b}$$

Now for certain ranges of γ and ν it will be possible to approximate the two functions of Eqs. (D-8a,b) by unity and zero respectively. The deviations will be worst for large σ, and in fact $g(\sigma)$ and $h(\sigma)$ approach limiting values as σ becomes infinite:

$$g(\infty) = \exp\left(-\frac{\gamma^3}{2\nu^2} + \ldots\right) \qquad \text{(D-9a)}$$

$$h(\infty) = \frac{\pi}{4}(\gamma^2/\nu)\left[1 - \frac{5}{8}(\gamma/\nu)^2 + \ldots\right] \quad . \qquad \text{(D-9b)}$$

The factor $g(\sigma)$ will be considered approximately unity if the exponent in Eq. (D-9a) is less than 0.1 or, equivalently,

$$\nu > 2.24\ \gamma^{3/2} \quad \text{(Criterion C)} \quad . \qquad \text{(D-10)}$$

On the other hand, a term in $h(\sigma)$ will be neglected if it is less than 0.1 radian. This condition, applied to the two terms of (D-9b) respectively, yields

$$\nu > 15.7\ \gamma^2 \quad \text{(Criterion D)} \qquad \text{(D-11)}$$

$$\nu > 1.70\ \gamma^{4/3} \quad \text{(Criterion E)} \quad . \qquad \text{(D-12)}$$

Criteria C and E are seen from Fig. D-1 to be less restrictive than Criterion A for values of γ which are of physical interest, while Criterion D is more restrictive only for $\gamma > 0.24$. Thus, we have for all cases of interest where the approximate solution is at all valid

$$g(\sigma) \approx 1 \qquad \text{(D-13a)}$$

$$h(\sigma) \approx (\gamma^2/2\nu)\ \tan^{-1}\sigma \quad , \qquad \text{(D-13b)}$$

and

$$u_1(\sigma) = \left|\sigma + \sqrt{1+\sigma^2}\right|^{\gamma} \exp\left\{i\nu\left[\sigma + \frac{1}{2}(\gamma/\nu)^2 \tan^{-1}\sigma\right]\right\} \qquad \text{(D-14a)}$$

$$u_2(\sigma) = \left|\sigma + \sqrt{1+\sigma^2}\right|^{-\gamma} \exp\left\{-i\nu\left[\sigma + \frac{1}{2}(\gamma/\nu)^2 \tan^{-1}\sigma\right]\right\} \quad . \qquad \text{(D-14b)}$$

APPENDIX E

APPROXIMATE METHOD FOR THE COMPUTATION OF $u_s(\sigma)$ FOR THE EXPERIMENTAL SYSTEM

APPENDIX E

APPROXIMATE METHOD FOR THE COMPUTATION OF $u_3(\sigma)$ FOR THE EXPERIMENTAL SYSTEM

The computation of $u_3(\sigma)$ depends upon the finding of a particular integral of Eqs. (56a,b). If the inequality of Eq. (57) holds, then this system of equations can be written as follows:

$$x'' + \nu^2 x = (1 + \sigma^2)^{-1/2} \qquad \text{(E-1a)}$$

$$y'' + \nu^2 y = (1 + \sigma^2)^{-1/2} x \quad . \qquad \text{(E-1b)}$$

Over the range of values of σ which are of interest in the current problem—*i.e.*, $0 \leqslant \sigma \leqslant 19$, the right-hand side of (E-1a) can be represented quite well by the following exponential function:

$$(1 + \sigma^2)^{-1/2} \approx 0.708\ \epsilon^{-0.622\sigma} + 0.292\ \epsilon^{-0.1135\sigma} + 0.440\ \sigma\ \epsilon^{-1.898\sigma} \quad . \qquad \text{(E-2)}$$

Figure (E-1) shows the original function and the approximation of Eq. (E-2) for purposes of comparison. It is seen that the approximation is very good in the most important region, near the lower end of the wire, while it deteriorates somewhat for values of σ above about 10.

Use of Eq. (E-2) in Eq. (E-1a) leads to the following:

$$x(\sigma) = \frac{0.708}{0.3865 + \nu^2}\ \epsilon^{-0.622\sigma} + \frac{0.292}{0.01289 + \nu^2}\ \epsilon^{-0.1135\sigma}$$

$$+ \frac{0.440}{3.60 + \nu^2} \left(\frac{3.80}{3.60 + \nu^2} + \sigma \right) \epsilon^{-1.898\sigma} \quad . \qquad \text{(E-3)}$$

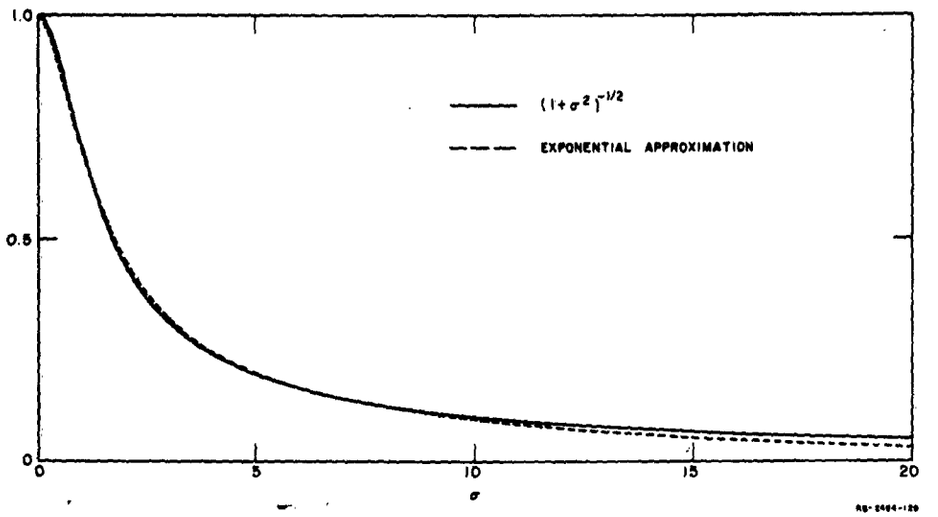

FIG. E-1
EXPONENTIAL APPROXIMATION FOR $(1+\sigma^2)^{-1/2}$

It is then possible, for each value of ν, to obtain graphically an approximate expression for $(1 + \sigma^2)^{-1/2} x(\sigma)$. For the case at hand, an expression of the form

$$(1 + \sigma^2)^{-1/2} x(\sigma) \approx a(\nu) \epsilon^{-b(\nu)\sigma} \qquad \text{(E-4)}$$

yields sufficiently good results. Substitution of Eq. (E-4) into Eq. (E-1b) leads to the following expression for $y(\sigma)$:

$$y(\sigma) = \frac{a(\nu)}{[b(\nu)]^2 + \nu^2} \epsilon^{-b(\nu)\sigma} \qquad \text{(E-5)}$$

The complete solution $u_3(\sigma)$ is then easily obtained from Eq. (55). Results for $\nu = 1, 2, 3$ are shown in Fig. 8 of the main body of this report.

ACKNOWLEDGMENT

The author is deeply indebted to Dr. R. L. Tanner, without whose ideas, suggestions, and moral support this work would have been impossible. To Mr. E. E. Spitzer must go the credit for the detailed design of the end-weights. Many thanks are due also to the Mathematics Department for their capable assistance in performing many of the numerical computations.

REFERENCES

1. J. V. N. Granger, "Wing and Tail Cap Antennas," Tech. Report 6, Contract AF 19(122)-78, SRI Project 188, Stanford Research Institute, Menlo Park, California (March 1950).

2. J. V. N. Granger and J. T. Bolljahn, "Aircraft Antennas," *Proc. IRE* 43, 12, pp. 533-550 (May 1955).

3. R. L. Tanner, "Shunt-Fed and Notch-Fed Aircraft Antennas," Tech. Report 61, Contract AF 19(604)-1296, SRI Project 1197, Stanford Research Institute, Menlo Park, California (July 1957).

4. G. Birkhoff and E. H. Zarantonello, *Jets, Wakes, and Cavities*, pp. 280-294 (Academic Press, Inc., New York, N.Y., 1957).

5. W. H. Phillips, "Theoretical Analysis of Oscillations of a Towed Cable," Tech. Note 1796, National Advisory Committee for Aeronautics, Washington, D. C. (January 1949).

6. W. Schwartzapfel, "Investigation of the Aerodynamic Characteristics of Trailing Antennas at High Speeds," Report CC-551-G-5, Contract W33-038 ac-20197, Cornell Aeronautical Laboratory, Inc., Buffalo, New York (15 March 1950).

7. W. H. Phillips, "Stability of a Body Stabilized by Fins and Suspended from an Airplane," Advance Restricted Report L4D18, National Advisory Committee for Aeronautics, Washington, D. C. (April 1944).

8. H. C. Plummer, "On the Form of the Trailing Aerial," *Phil. Mag.*, Series 6, 38, 228, pp. 732-736 (December 1919).

9. "Investigation of the Aerodynamic Characteristics of Trailing Antennas at High Speeds," Quarterly Engineering Report CC-551-G-1, Contract W33-038 ac-20197, Cornell Aeronautical Laboratory, Inc., Buffalo, New York (10 August 1948).

10. R. T. Jones, "Effects of Sweepback on Boundary Layer and Separation," Tech. Note 1402, National Advisory Committee for Aeronautics, Washington, D. C. (July 1947).

11. L. Prandtl and O. G. Tietjens, *Applied Hydro- and Aeromechanics*, pp. 96-99 (Dover Publications, Inc., New York, N. Y., 1957).

12. F. E. Gowen and E. W. Perkins, "Drag of Circular Cylinders for a Wide Range of Reynolds Numbers and Mach Numbers," Tech. Note 2960, National Advisory Committee for Aeronautics, Washington, D. C. (June 1953).

TECHNICAL REPORTS IN THIS SERIES

Reports Issued on Contract AF 19(122)-78

1. "Electric Dipoles in the Presence of Elliptic and Circular Cylinders," by W. S. Lucke, September 1949.

2. "Asymmetrically Fed Antennas," by C. T. Tai, November 1949.

3. "Double-Fed and Coupled Antennas," by C. T. Tai, February 1949.

4. "Equivalent Radii of Thin Cylindrical Antennas with Arbitrary Cross Sections," by Carson Flammer, March 1950.

5. "Use of Complementary Slots in Aircraft Antenna Impedance Measurements," by J. T. Bolljahn, February 1950.

6. "Wing-Cap and Tail-Cap Aircraft Antennas," by J. V. N. Granger, March 1950.

7. "Investigation of Current Distribution on Asymmetrically-Fed Antennas by Means of Complementary Slots," by R. M. Hatch, Jr., February 1950.

8. "Electromagnetic Resonance Phenomena in Aircraft Structures," by A. S. Dunbar, May 1950.

9. "The Effect of a Grounded Slab on the Radiation from a Line Source," by C. T. Tai, June 1950.

10. "A Method for the Calculation of Progressive-Phase Antennas for Shaped Beams," by A. S. Dunbar, June 1950.

11. "Admittance of an Open-Ended Coaxial Line in an Infinite Grounded Plane," by W. S. Lucke, June 1950.

12. "A Variational Solution to the Problem of Cylindrical Antennas," by C. T. Tai, August 1950.

13. "Uniform Progressive-Phase Antennas Having Asymmetrical Amplitude Distributions," by A. S. Dunbar, September 1950.

14. "Small Dipole-Type Antennas," by J. T. Bolljahn, September 1950.

15. "Tables of Modified Cosine Integrals," January 1951.

16. "Prolate Spheroidal Wave Functions," by Carson Flammer, February 1951.

TECHNICAL REPORTS IN THIS SERIES

Reports Issued on Contract AF 19(122)-78

1. "Electric Dipoles in the Presence of Elliptic and Circular Cylinders," by W. S. Lucke, September 1949.

2. "Asymmetrically Fed Antennas," by C. T. Tai, November 1949.

3. "Double-Fed and Coupled Antennas," by C. T. Tai, February 1949.

4. "Equivalent Radii of Thin Cylindrical Antennas with Arbitrary Cross Sections," by Carson Flammer, March 1950.

5. "Use of Complementary Slots in Aircraft Antenna Impedance Measurements," by J. T. Bolljahn, February 1950.

6. "Wing-Cap and Tail-Cap Aircraft Antennas," by J. V. N. Granger, March 1950.

7. "Investigation of Current Distribution on Asymmetrically-Fed Antennas by Means of Complementary Slots," by R. M. Hatch, Jr., February 1950.

8. "Electromagnetic Resonance Phenomena in Aircraft Structures," by A. S. Dunbar, May 1950.

9. "The Effect of a Grounded Slab on the Radiation from a Line Source," by C. T. Tai, June 1950.

10. "A Method for the Calculation of Progressive-Phase Antennas for Shaped Beams," by A. S. Dunbar, June 1950.

11. "Admittance of an Open-Ended Coaxial Line in an Infinite Grounded Plane," by W. S. Lucke, June 1950.

12. "A Variational Solution to the Problem of Cylindrical Antennas," by C. T. Tai, August 1950.

13. "Uniform Progressive-Phase Antennas Having Asymmetrical Amplitude Distributions," by A. S. Dunbar, September 1950.

14. "Small Dipole-Type Antennas," by J. T. Bolljahn, September 1950.

15. "Tables of Modified Cosine Integrals," January 1951.

16. "Prolate Spheroidal Wave Functions," by Carson Flammer, February 1951.

17. "An Antenna Evaluation Method," by W. S. Lucke, April 1951.

18. "Radar Response from Thin Wires," by C. T. Tai, March 1951.

19. "The Measurement of Low-Frequency Aircraft Antenna Properties Using Electrostatic Methods," by J. T. Bolljahn, September 1951.

20. (Dropped).

21. "A Method for the Calculation of Progressive-Phase Antennas for Shaped Beams," Part II, by A. S. Dunbar, May 1951.

22. "The Prolate Spheroidal Monopole Antenna," by Carson Flammer, August 1957, issued on Contract AF 19(604)-1296.

23. "Variational Solution for the Problem of the Asymmetric Dipole," by I. Reese, August 1951.

24. "Quasi-Static Solution for Diffraction of a Plane Electromagnetic Wave by a Small Oblate Spheroid," by C. T. Tai, September 1952 [Issued on Contract AF 19(604)-266].

25. "Transmission Through a Rectangular Aperture in an Infinite Screen," by W. S. Lucke, September 1951.

Reports Issued on Contract AF 19(604)-266

26. "Improvements in Instrumentation for the Investigation of Aircraft Antenna Radiation Patterns by Means of Scale Models," by R. M. Hatch, Jr., August 1952.

27. "The Vector Wave Solution of the Diffraction of Electromagnetic Waves by Circular Disks and Apertures," by Carson Flammer, September 1952.

28. "An Investigation of the Distribution of Current on Collinear Parasitic Antenna Elements," by R. M. Hatch, Jr., August 1952.

29. "On the Theory of Diffraction of Electromagnetic Waves by a Sphere," by C. T. Tai, October 1952.

30. "High-Frequency Airborne Direction Finding," by P. S. Carter, Jr., December 1952.

31. "An Electrolytic Tank Method for Low-Frequency Loop Antennas Studies," by R. F. Reese, July 1953.

32. "Radiation from a Uniform Circular Loop Antenna in the Presence of a Sphere," by C. T. Tai, December 1952.

33. "A Computer for Use with Antenna Model Ranges," by C. E. Fisher, February 1953.

34. "Tail-Cap Antenna Radiation Pattern Studies," by J. H. Bryan, January 1953.

35. "U-H-F Tail-Cap Antenna Pattern Characteristics and Their Control," by A. R. Ellis, March 1955 [issued on Contract AF 19(604)-1296].

36. "Mutual Admittance of Slots in Cylinders," by W. S. Lucke, February 1953.

37. Radio Interference from Corona Discharges," by R. L. Tanner, April 1953.

38. "Effects of Airframe Configuration on Low-Frequency Antenna Characteristics," by C. M. Hoblitzell, April 1953.

39. "The Effects of Thin Resistive Coatings on Low-Frequency Aircraft Antenna Performance," by C. W. Steele [issued on Contract AF 19(604)-1296] January 1956.

40. "Analysis of the Overstation Behavior of Airborne ADF Systems," by H. H. Ward, June 1954.

41. "Some Electromagnetic Problems Involving a Sphere," by C. T. Tai, April 1953.

42. "Radiation Pattern Measurements of Stub and Slot Antennas on Spheres and Cylinders," by J. Bain, April 1953.

43. "Current Distribution on Wing-Cap and Tail-Cap Antennas," by Irene C. Carswell, May 1954.

44. "A Study of Radiating Structures for Perpendicularly-Polalized Flush Radar Antennas," by Edward M. T. Jones and Seymour B. Cohn, July 1953.

45. "Radiation from Current Elements and Apertures in the Presence of a Perfectly Conducting Half-Plane Sheet," by C. T. Tai, July 1954.

46. "A Glossary of Dyadic Green's Functions," by C. T. Tai, July 1954.

47. "Horizontally Polarized Long-Slot Array," by R. C. Honey, August 1954.

Reports Issued on Contract AF 19(604)-1296

48. "Microwave Radiation from Large Finite Bodies," by Seymour B. Cohn and Tetsu Morita, January 1955.

49. "Radiation from Electric and Magnetic Dipoles in the Presence of a Conducting Circular Disk," by Carson Flammer, February 1955.

50. "A Study of Some Inherent Errors in the Three-Dimensional Raydist System," by Irene Carswell, March 1955.

51. "Operating Characteristics of Flush-Mounted Bombing Antennas," by E. M. T. Jones, November 1955.

52. "Properties of the Asymmetric Dipole," by Irene Carswell, December 1955.

53. "Notch Coupling to the Electromagnetic Resonances of a Delta-Wing Aircraft," by William L. Jones, December 1955.

54. "A Flush-Mounted, Horizontally Polarized Directional Antenna," by R. C. Honey, January 1956.

55. "Radiation from a Flush-Mounted Scanning Antenna on the Nose Section of a Supersonic Aircraft," by J. K. Shimizu and T. Morita, December 1955.

56. "An Economical Logarithmic Recording System," by Lloyd A. Robinson, June 1956.

57. "Variational Formulae for Domain Functionals in Electromagnetic Theory," by Carson Flammer, March 1957.

58. "Systems Considerations for High Speed Missile Seeker Antennas," by Donald L. Margerum and E. Thomas Brandon, May 1957. Confidential.

59. "High-Strength Dielectric Materials for Very Fast Aircraft," by Henry J. Sang, March 1957.

60. "Impedance Matching Limitations with Application to the Broadband Antenna Problem," by Arthur Vassiliadis, January 1957.

61. "Shunt-Fed and Notch-Fed H-F Aircraft Antennas," by Robert L. Tanner, July 1957.

62. "A Study of Precipitation-Static Noise Generation in Aircraft Canopy Antennas," by Joseph E. Nanevicz, September 1957.

63. "Electromagnetic Wave Propagation in a Medium with Variable Dielectric Constant $1 + kr^{-1}$," by Carson Flammer, January 1958.

64. "The Back-Scattering Cross Sections of Missile Trails," Flammer, June 1958.

65. "Ray-Tracing and Diffraction in a Medium with Variable P and Attenuation," by James A. Cochran, October 1958.

66. "Feasibility Study of Aircraft Antennas for Forward-Scat Meteor-Burst Communication," by J. F. Cline, July 1959.

67. "A Study of Possibilities for Improving Space Utilizatio Performance of Rhombic Antennas," by Angel Martin-Caloto

68. "Aerodynamic Characteristics of Trailing-Wire Antennas a sonic Speeds," by F. B. Harris, Jr., March 1960.